

## Research paper

## Distribution of Dinoflagellate cyst assemblages and palynofacies in the Upper Cretaceous deposits from the neritic Bou Lila section, External Rif (northwestern Morocco): Implications for the age, biostratigraphic correlations and paleoenvironmental reconstructions

Hamid Slimani<sup>a,\*</sup>, Victorien Michael Benam<sup>a,c</sup>, Daniel Țabără<sup>b</sup>, Habiba Aassoumi<sup>c</sup>, Hassan Jbari<sup>a</sup>, Mouna Chekar<sup>a</sup>, Imane Mahboub<sup>a</sup>, Amel M'Hamdi<sup>d</sup>

<sup>a</sup> Geo-Biodiversity and Natural Patrimony Laboratory (GEOBIO), "Geophysics, Natural Patrimony and Green Chemistry" Research Center (GEOPAC), Department of Earth Sciences, Scientific Institute, Mohammed V University in Rabat, Avenue Ibn Batouta, P.B. 703, 10106 Rabat-Agdal, Morocco

<sup>b</sup> Al. I. Cuza" University of Iași Department of Geology, 20A Carol I Blv., 700505 Iași, Romania

<sup>c</sup> Laboratory of Cartography and Digital Technology, Department of Earth Sciences, Faculty of Sciences, University Abdelmalek Essaâdi, Tétouan, Morocco

<sup>d</sup> Department of Geology, Faculty of Sciences of Tunis, University El Manar, "Campus Universitaire", 2092, El Manar II, Tunisia



## ARTICLE INFO

## Keywords:

Campanian dinoflagellate cysts  
Biostratigraphy  
Paleoenvironment  
Palynofacies  
Western External Rif  
Morocco

## ABSTRACT

As a part of our palynological investigations of the Upper Cretaceous deposits from the Rif Chain, the present study of the dinoflagellate cyst assemblage distribution and palynofacies was carried out in the Bou Lila section, located northeast of the city of Ksar El-Kébir (External Rif, northwestern Morocco). The study focused on the age refinement and interpretation of paleoenvironmental conditions within the basin during the sediment deposition. The analyzed samples are rich in palynomorphs, formed essentially of diverse and well-preserved dinoflagellate cysts, which are associated with phytoclasts and rare microforaminiferal test linings, spores, pollen grains and algae.

The Bou Lila section is assigned to the late Campanian, based on dinoflagellate cyst taxa, whose first appearance datums (FADs) or last appearance datums (LADs) are markers of the late Campanian. These taxa include *Areoligera coronata*, *Areoligera senonensis*, *Cerodinium diebelii*, *Chatangiella? robusta*, *Cribroperidinium wilsonii* subsp. *wilsonii*, *Impagidinium rigidaseptatum*, *Odontochitina operculata*, *Odontochitina costata*, *Palynodinium grillator*, *Raetiaedinium belgicum*, *Rigaudella appenninica*, *Trichodinium castanea* subsp. *castanea*, *Trigonopyxidina ginella*, *Trithyrodonium evittii*, *Trithyrodonium suspectum*, *Xenascus ceratioides* and *Xenascus wetzeli*. The high diversity of the dinoflagellate cyst taxa made it possible to correlate the Bou Lila section with biostratigraphically well-calibrated upper Campanian sequences from several Tethyan and also Boreal sites, including the type Campanian area and the GSSP for the base of the Maastrichtian in southwestern France and the type Maastrichtian area in Limburg.

The fluctuations in the relative abundances of the selected dinoflagellate cyst groups and other quantitative palynological parameters allow a recognition of three paleoecological zones. They indicate a gradual passage from an inner neritic setting, with high productivity conditions in the most basal part of the section, to a stable outer neritic setting in the upper part of the section.

The palynofacies analyses are in general agreement with the dinoflagellate cyst results, indicating a passage from a proximal depositional environment in the lowermost part of the section to a distal depositional environment in the uppermost part of the section. The dinoflagellate cyst assemblage indicates a subtropical to temperate setting, with the presence of the northern high-latitude cold-water species *Palynodinium grillator*, suggesting a short cooling episode or also conditions of water stratification during the late Campanian.

\* Corresponding author.

E-mail address: [hamid.slimani@um5.ac.ma](mailto:hamid.slimani@um5.ac.ma) (H. Slimani).

<https://doi.org/10.1016/j.marmicro.2020.101951>

Received 28 July 2020; Received in revised form 22 October 2020; Accepted 6 December 2020

Available online 9 December 2020

0377-8398/© 2020 Elsevier B.V. All rights reserved.

## 1. Introduction

This study of the distribution of dinoflagellate cysts and palynofacies is carried out using the marly succession, assigned previously to the Upper Cretaceous in the geological map of the Rif Chain (1:500,000) by Suter (1980a, 1980b). Paleogeographically, the Late Cretaceous is known by worldwide marine provinces, characterized by typical climates and biota. Connections between these marine provinces were marked by migrating organisms, controlled by oceanic thermohaline circulations and climatic changes (Luyendyk et al., 1972; Barrón, 1987; Michaud, 1987; Hay, 2009). The latest Cretaceous greenhouse time, notably the Campanian and the Maastrichtian, was characterized by a progressive global cooling with superimposed cool/warm fluctuations (e.g., Thibault et al., 2015).

Although dinoflagellates are planktonic organisms, characterized by a wide geographic distribution, certain taxa reflect a provincialism. Three paleobiogeographic provinces were defined by Lentin and Williams (1980), based on the latitudinal distribution of Campanian organic-walled dinoflagellate cysts: a tropical to subtropical province, a temperate province and a boreal province. The southward migration of dinoflagellates (e.g., *Palynodinium grillator*) caused by cooling events (Brinkhuis et al., 1998; Slimani et al., 2010; Chakir et al., 2020; Jbari et al., 2020) and northward migration (e.g., *Trithyrodinium evittii*) caused by warming events (Smit and Brinkhuis, 1996; Nøhr-Hansen and Dam, 1997) during the Campanian–Danian interval, were reported mainly in the Northern Hemisphere. Calcareous nannofossils and foraminifera reflect also fluctuations in sea-surface temperatures during this interval in the boreal sea and tropical South Atlantic and Pacific oceans, showing notably a warming during the late Campanian and cooling across the Campanian–Maastrichtian boundary (Thibault and Gardin, 2010; Thibault et al., 2015, 2016).

Dinoflagellate cysts are widely distributed from inner neritic to

oceanic settings. Therefore, they have proven to be very useful for biostratigraphic and paleoenvironmental interpretations and effective in our previous palynological studies of the Rif Chain (Slimani et al., 2008, 2010, 2012, 2016, 2019; Slimani and Toufiq, 2013; Guédé et al., 2014; Guédé, 2016; Chekar et al., 2016, 2018; Mahboub et al., 2019; Jbari et al., 2020; Mahboub and Slimani, 2020). The palynofacies analysis constitutes another tool, which is relevant for paleoenvironmental reconstructions (e.g., Tyson, 1995).

The first studies of Campanian dinoflagellate cyst assemblages, undertaken in the Rif Chain, include studies of Guédé (2016) and Slimani et al. (2016) in the Sekada section (~40 km northeast of the study area) and also Jbari et al. (2020) in the Tattofte section (~6 km south of the study area). They aimed to provide paleobiogeographic interpretations and age control and refinement of deposits, assigned previously to the Upper Cretaceous in the geological map of the Rif Chain (1:500,000) by Suter (1980a) (Fig. 2B).

The Bou Lila outcrop consists of a marly succession, which was also assigned previously to the Upper Cretaceous by Suter (1980a). The goals of this paper are:

- 1) to refine the geological age of the sampled marly succession and correlate it with other Tethyan and Boreal sequences;
- 2) to present new paleoenvironmental data and interpretations and compare the paleoenvironments suspected from fluctuations in the relative abundances of selected ecological groups of dinoflagellate cysts with those revealed by palynofacies analyses;
- 3) and to place the study area in a paleobiogeographic setting;

## 2. Regional setting

The Bou Lila section is located geographically in the Ksar El-Kébir region, northwestern Morocco (Fig. 1), and geologically in the

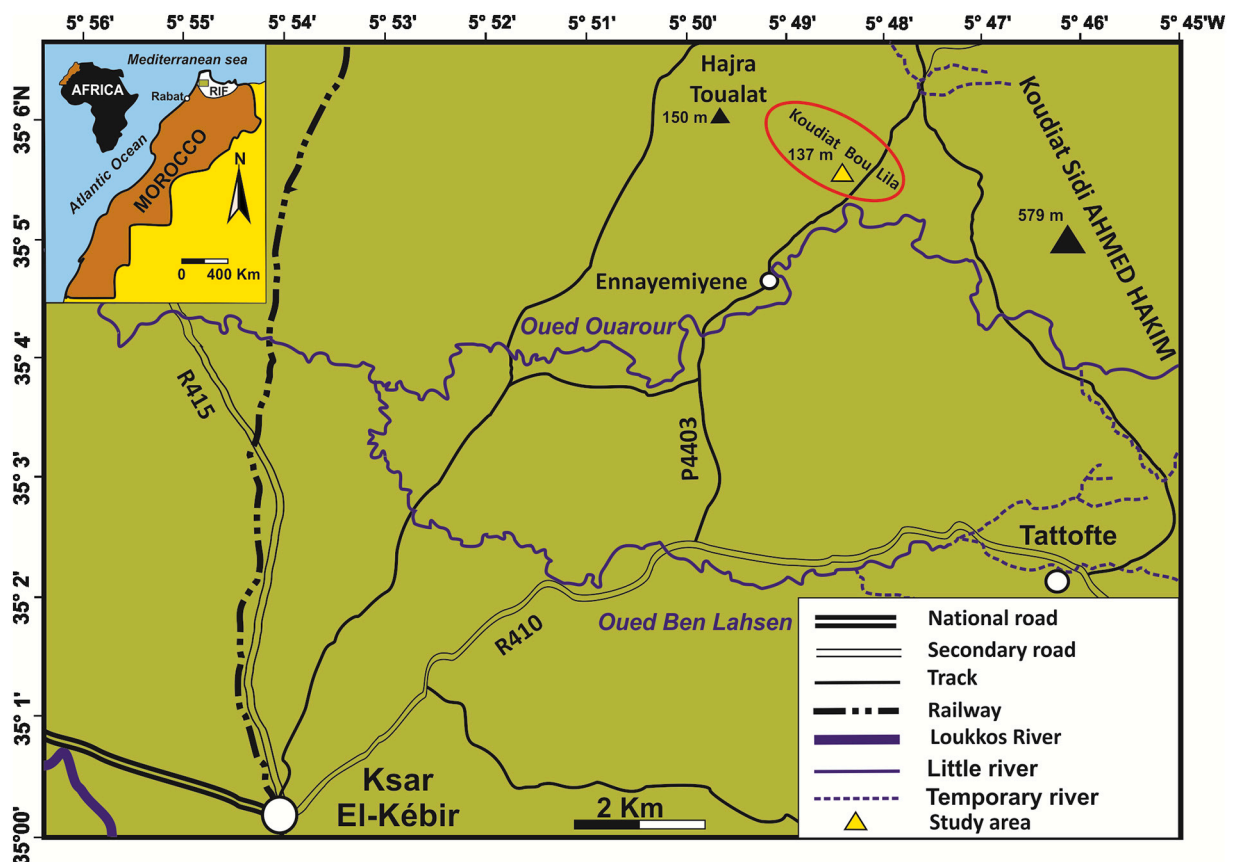


Fig. 1. Location map of the Bou Lila section, region of Ksar El-Kébir, northwestern Morocco.

southwestern border of the western External Rif Chain and northeastern border of the Gharb Plain (Fig. 2A). The Rif Chain constitutes the westernmost part of the Alpine Belt and an important part of the betico-rifo-tellian chains, which are the result of the rapprochement and a collision between the African and European plates during the progressive opening of the Atlantic Ocean from the Jurassic to the Present

(Patriat et al., 1982; Michard et al., 2002). The Rif Chain is subdivided into three main structural domains with Mesozoic and Cenozoic deposits (Fig. 2A), exposed from the north to the south: the Internal Rif or Alboran Domain, the Maghrebien Flysch Nappes and the External Rif (Suter, 1980a, 1980b; Chalouan et al., 2001). From the north to the south, the External Rif is structured into three zones, namely: the

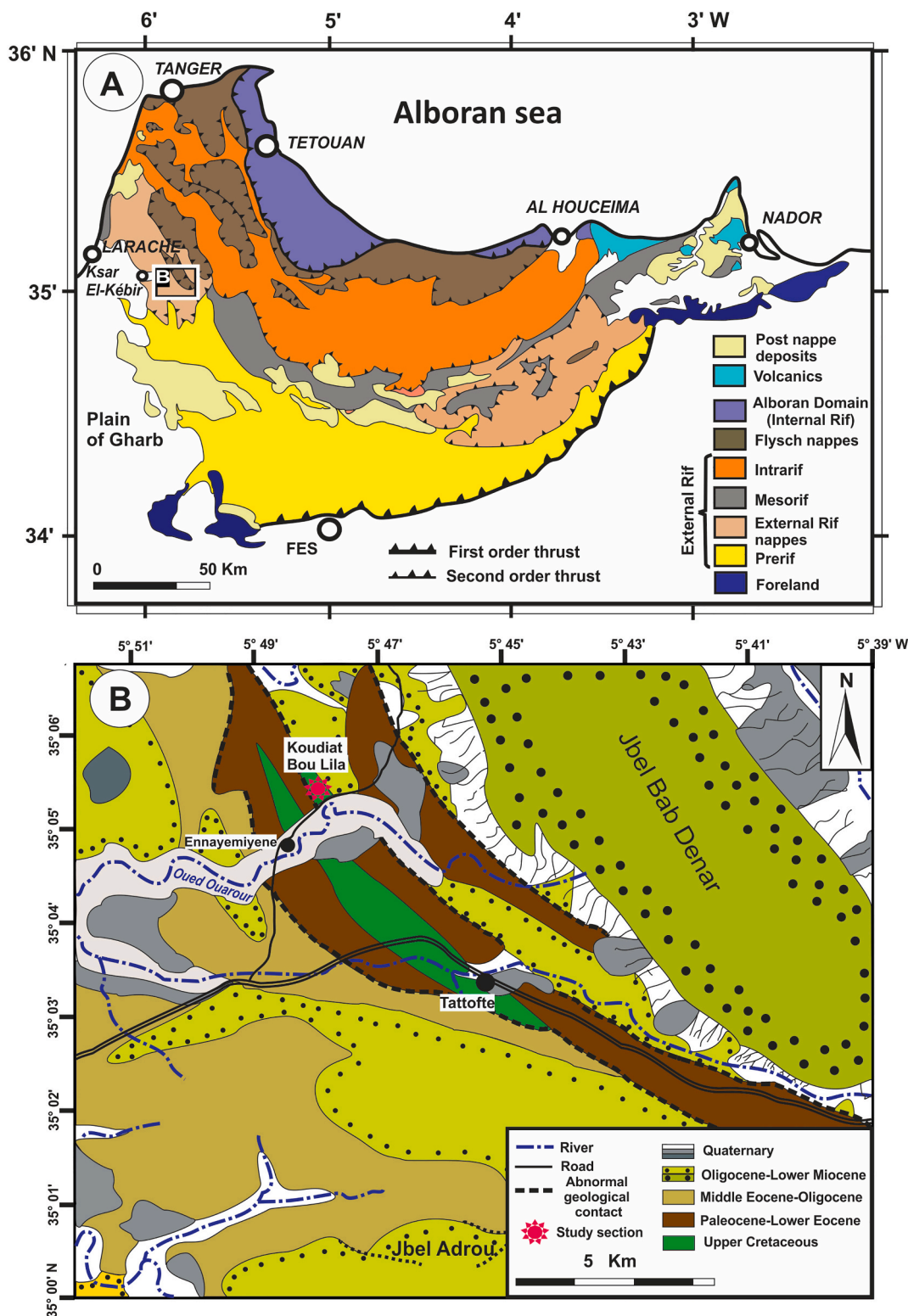


Fig. 2. Simplified structural map of the Rif Chain (A), modified after Michard et al. (2008), and geological setting of the Bou Lila section, region of Ksar El-Kébir, western External Rif, northwestern Morocco (B), adapted from the geological map of Rif at 1:500,000 (Suter, 1980a).



Intrarif, the Mesorif and the Prerif (Leblanc, 1975–1979; Suter, 1980a, 1980b).

The Bou Lila sequence is considered as a part of the Habt Unit (Suter, 1980a, 1980b; Chalouan et al., 2001). It is located in the Koudiat Bou Lila (35° 5'7.50"N, 5° 48'40.92"W), approximately 14 km northeast of the city of Ksar El-Kébir and 2 km northeast of the village of Ennaye-miyene (Fig. 1). It is exposed about 300 m from the right bank of the Ouarour River. From a lithological point of view, the section consists of an approximately 14-m thickness of marls, which alternate with marly limestone beds of decimetric thickness. From the base to the top, the section is composed of 3.8-m thickness of yellowish marls, followed by a 1 m transitional interval of alternating decimetric yellowish and grey marly layers, which is overlain by 5.7 m thick of grey marls (Figs. 3, 6). From the base to the top of the section, fifteen rock samples were collected, including 5 samples (KBL1–KBL5) every 100 cm in the Yellowish marls, 7 samples (KBL6–KBL12) every 10–25 cm in the yellowish-grey marly transition, and 3 samples (KBL13–KBL15) every 1–2.5 m in the grey marls (Fig. 6).

### 3. Methods

#### 3.1. Sample preparation

The fifteen samples were processed following standard palynological preparation techniques. The processing involved an initial treatment of 40 g of sediment with cold hydrochloric acid (HCl, 20%), followed by two successive treatments for 96 h in cold hydrofluoric acid (HF, 40%) in order to dissolve carbonates and silicates, respectively. Samples were neutralized with distilled water between the acid treatments. The

remaining material was treated in hot HCl (20%) for 20 min in order to remove silicofluorides produced during the hydrofluoric acid treatment. The organic residues were sieved on a nylon screen with a mesh size of 15 µm and mounted in glycerine jelly on two microscope slides.

The palynological slides were studied, using a transmitted light microscope (Olympus BX53), equipped with a digital camera Olympus C-400 Zoom. All the slides are kept in the botanical collection of the National Herbarium of Rabat (RAB), Scientific Institute, University Mohammed V, Rabat (Morocco). The England Finder (EF) coordinates of the figured specimens are given in the captions of the Plates 1–4. The nomenclature of dinoflagellate cyst taxa and references to their authors are based on the Lentin and Williams Index (Williams et al., 2017).

Carbonate analyses were performed according to standard AFNOR (1996), which uses the acid attack and the CO<sub>2</sub> measurement method.

#### 3.2. Approaches of study

Biostratigraphic and paleoenvironmental interpretations are mainly based on dinoflagellate cyst analyses. Palynofacies are used as additional tool for paleoenvironmental reconstructions.

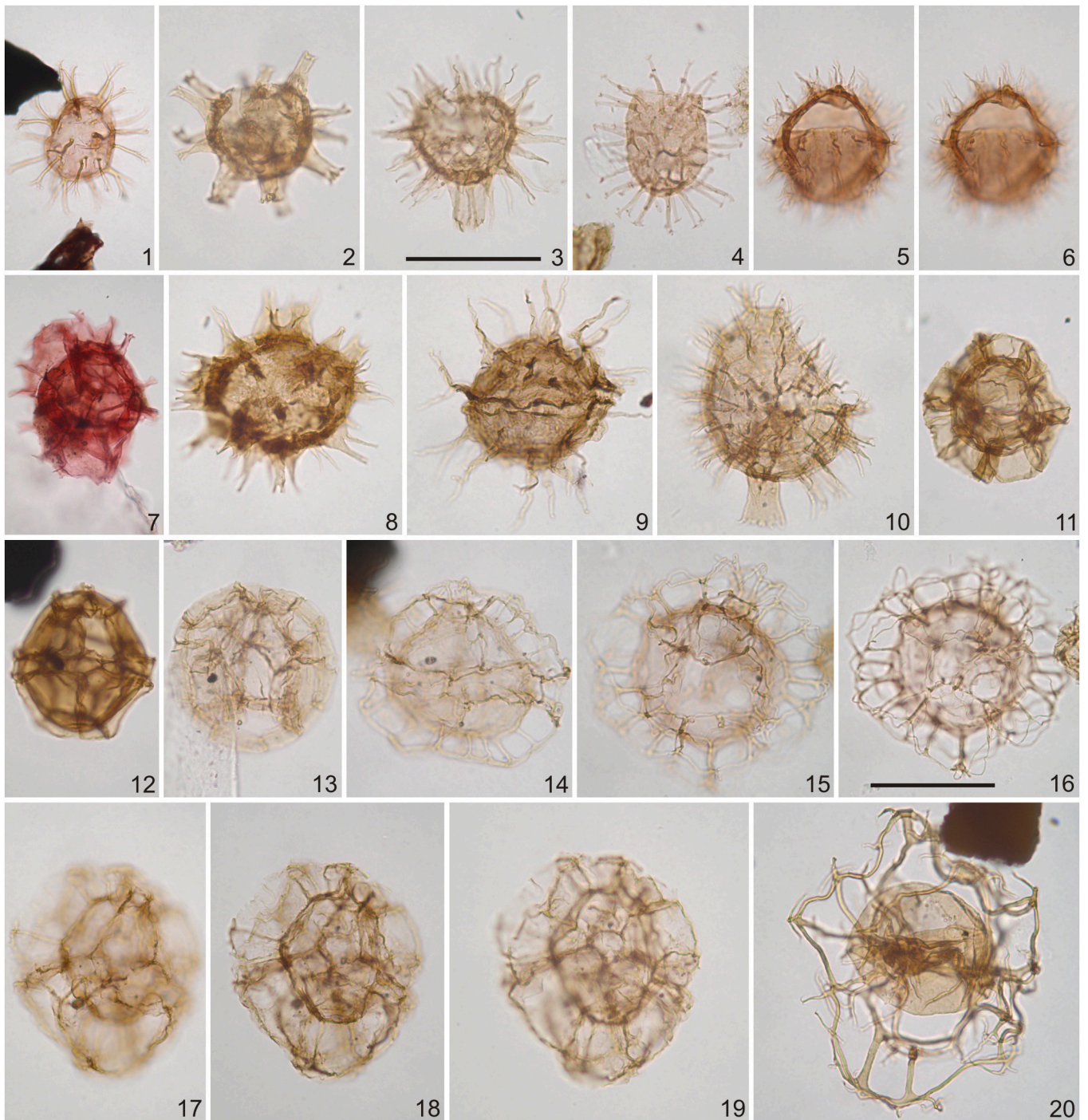
The age determinations are here based mainly on the first appearance datums and last appearance datums of dinoflagellate cyst taxa, previously considered as biostratigraphic markers. For paleoenvironmental reconstructions, we used the following quantitative parameters (cf. Versteegh, 1994; Guasti, 2005):

- 1) the relative abundance (%) of dinoflagellate cyst groups that are often considered as paleoenvironmental indicators;



**Fig. 3.** Photographs of the Bou Lila outcrop, region of Ksar El-Kébir, western External Rif, northwestern Morocco. A, B part of the channel, in which the samples were collected; C. transition yellowish-grey marls; D. grey marls.





(caption on next page)

**Plate 1.** Campanian dinoflagellate cysts from the Bou Lila outcrop, western External Rif, northwestern Morocco. Scale bars represents 40  $\mu\text{m}$ .

1. *Surculosphaeridium longifurcatum*; sample KBL6, slide 2, EF J38; focus on processes.
2. *Florentinia aculeata*; sample KBL13, slide 1, EF R23; focus on the archeopyle (combination of the precingular 3" and apical plates).
3. *Diphyes colligerum*; sample KBL13, slide 2, EF K46/2; focus on the antapical horn and processes.
4. *Tanyosphaeridium xanthiopyxides*; sample KBL 6, slide 2, EF J49/1; focus on the wall surface and processes.
- 5, 6. *Raetiaedinium belgicum*; sample KBL5, slide 2, EF X34; successive foci, showing the precingular archeopyle type 2P, the apical bulge and processes.
7. *Rottnestia wetzelii* subsp. *brevispinosa*; sample KBL4, slide 2, EF P54; focus on the two pericoels.
8. *Florentinia ferox*; sample KBL15, slide 1, EF; B40/3.
9. *Hystrichodinium pulchrum*; sample KBL13, slide 1, EF G21/2.
10. *Coronifera oceanica*; sample KBL7, slide 2, EF U35/2.
11. *Pterodinium cretaceum*; sample KBL15, slide 1, EF P43/3.
12. *Impagidinium cristatum*; sample KBL14, slide 1, EF J46/1; focus on sutural septa.
13. *Impagidinium* sp. of Slimani et al. (2016); sample KBL6, slide 2, EF R42/2; focus on sutural septa.
14. *Unipontidinium grande*; sample KBL14, slide 1, EF X46; focus on the distal sutural trabeculae.
- 15, 16. *Nematosphaeropsis* sp. cf. *lativittata*; sample KBL7, slide 2, EF F56/2; 15, focus on the precingular archeopyle type P (3"), 16. ventral surface with focus on the penitabular trabeculae.
- 17–19. *Impagidinium rigidaseptatum*; sample KBL14, slide 1, EF M35/3; successive foci showing the distal margins of septa (17), precingular archeopyle type P(3") and ventral surface.
20. *Cannosphaeropsis utinensis*; sample KBL7, slide 2, EF K32/4.

- 2) the peridinioid/gonyaulacoid dinoflagellate cyst ratios (P/G) [ $(P/G) = nP/(nP+nG)$ ];
- 3) the sporomorph (spores and pollen grains)/dinoflagellate cyst (dinoflagellate cysts and marine acritarchs) ratios (S/D) [ $S/D = nS/(nD+nS)$ ];
- 4) and the inner neritic dinoflagellate cyst/outer neritic to oceanic dinoflagellate cyst ratios (IN/ON) [ $IN/ON = nIN/(nIN+nON)$ ] (Table 3, Fig. 6).

The relative abundances (%) of each group of dinoflagellate cysts are calculated in relation to the total of 400 specimens of dinoflagellate cysts per sample. They provide information on the environmental conditions, including oceanic environment, inner or outer neritic and lagoonal environment, as well as information on energy, bathymetry, salinity, temperature, nutrient supply, transgressive or regressive regime and oceanic circulation (Table 2). The S/D ratios provide information on the continental influence and changes in sea level (Versteegh, 1994; Pross, 2001; Guasti, 2005), thus an eventual presence of palynomorphs of continental origin in a marine environment would be due to a continental influence favored especially by river transport. The P/G ratios reveal changes in primary productivity in the geologic past, a peridinioid-dominated assemblage indicating nutrient-rich and low-salinity conditions (Versteegh, 1994; Guasti, 2005; Carvalho et al., 2016; Vieira and Jolley, 2020). The IN/ON ratios provide information on distance from land.

Other information regarding depths and energy conditions of the basin was obtained based on the carbonate analyses and lithology.

The palynofacies analysis is based on counting at least 500 palynodebris in each sample in order to obtain paleoenvironmental information, following Tyson (1995), Mendonça Filho et al. (2011) and McArthur et al. (2017). Three groups of the kerogen constituents were suggested in this study: (1) palynomorphs (spores, pollen grains, dinoflagellate cysts and algae), (2) phytoclasts (opaque and translucent organic particles derived from terrestrial plants) and (3) amorphous organic matter (AOM) which includes structureless organic components derived from phytoplankton or degraded higher plant debris. The palynofacies of the samples also includes small amounts of microforaminiferal test linings. The paleoenvironmental interpretations, revealed by the palynofacies composition, were compared with those inferred based on the relative abundance of the selected dinoflagellate cyst groups and the other parameters (P/G, S/D and IN/ON ratios).

#### 4. Previous studies on Campanian dinoflagellate cyst assemblages

Campanian dinoflagellate cyst assemblages were thoroughly studied in many regions of the Northern Hemisphere, especially in the

Campanian–Maastrichtian boundary sections.

The Campanian dinoflagellate cysts in Europe were first studied by Wilson (1971), who presented preliminary results of dinoflagellate distributions. He attempted to make biostratigraphic correlations between the Campanian deposits from the type Campanian area at Charente (southwestern France), the type Maastrichtian area of Limburg (Belgium and the Netherlands), southern Sweden and Denmark. Subsequently, Wilson (1974) proposed, in his unpublished PhD Thesis, three dinoflagellate cyst zones (Ia, Ib, II) for the upper Campanian chalk in the Maastricht area and Denmark, and Schumacker-Lamry (1977) suggested two dinoflagellate cyst zones Ia and Ib for the lower Campanian and upper Campanian chalks in the northeast of Belgium. Meanwhile, Foucher (1976, 1979) summarized the stratigraphic distribution of dinoflagellate cysts in the Campanian in the Paris Basin and northern Europe. Neumann et al. (1983), Masure (1985), Foucher (1983, 1985) restudied Campanian dinoflagellate cyst assemblages from the Campanian type area at Charente and the "Autoroute A10" in the Aquitaine Basin, and from the Maastrichtian type area, respectively. A new Campanian to Maastrichtian dinoflagellate cyst zonation was proposed by Kirsch (1991) in southern Germany. Slimani (1994, 1995, 1996, 2000, 2001a, 2001b, 2003) formally described more than 60 new species and 6 new genera of dinoflagellate cysts in the Campanian to Danian chalk in the Maastricht area and northern Belgium, proposed a new dinoflagellate cyst zonation and made biostratigraphical correlations with other elaborated scales in Western Europe. He proposed four new dinoflagellate cyst zones for the late Campanian: the *Exochosphaeridium? masureae*, *Hystrichokolpoma gamospina*, *Areoligera coronata* and *Samlandia mayi* zones, calibrated with the *Belemnitella mucronata*–*Belemnitella langei* zones of the conventional belemnite zonation and with the *Belemnitella woodi*–*Belemnitella minor* zones of NW Europe belemnite zonation. From these dinoflagellate cyst studies by Slimani, apparent contradictions in the dinoflagellate scale were resolved in several regions in the world. These studies, together with the revision of belemnites by Keutgen and Van der Tuuk (1990) and nannoplankton by Verbeek (1983), allowed the assignment of the Beutenaken Member to the upper Campanian, instead of lower Maastrichtian in its type locality. These changes lead to the removal of the inconsistencies between the stratotype of Beutenaken and other regions in the world (Slimani, 2001a). Therefore, several dinoflagellate cyst events, dated as early Maastrichtian in previous studies (e.g., last appearance datums of *Odontochitina operculata* and *Xenascus ceratioides*, first appearance datum of *Samlandia mayi*), have been moved from the early Maastrichtian to the latest Campanian. Slimani's dinoflagellate cyst zones proposed for the late Campanian, have been recognized in other regions in northern Europe and northern high latitudes, including Belgium (Slimani et al., 2011; Slimani and Louwey, 2011, 2013), Denmark (Surluk et al., 2013), Poland (Niechwedowicz, 2019), and Central



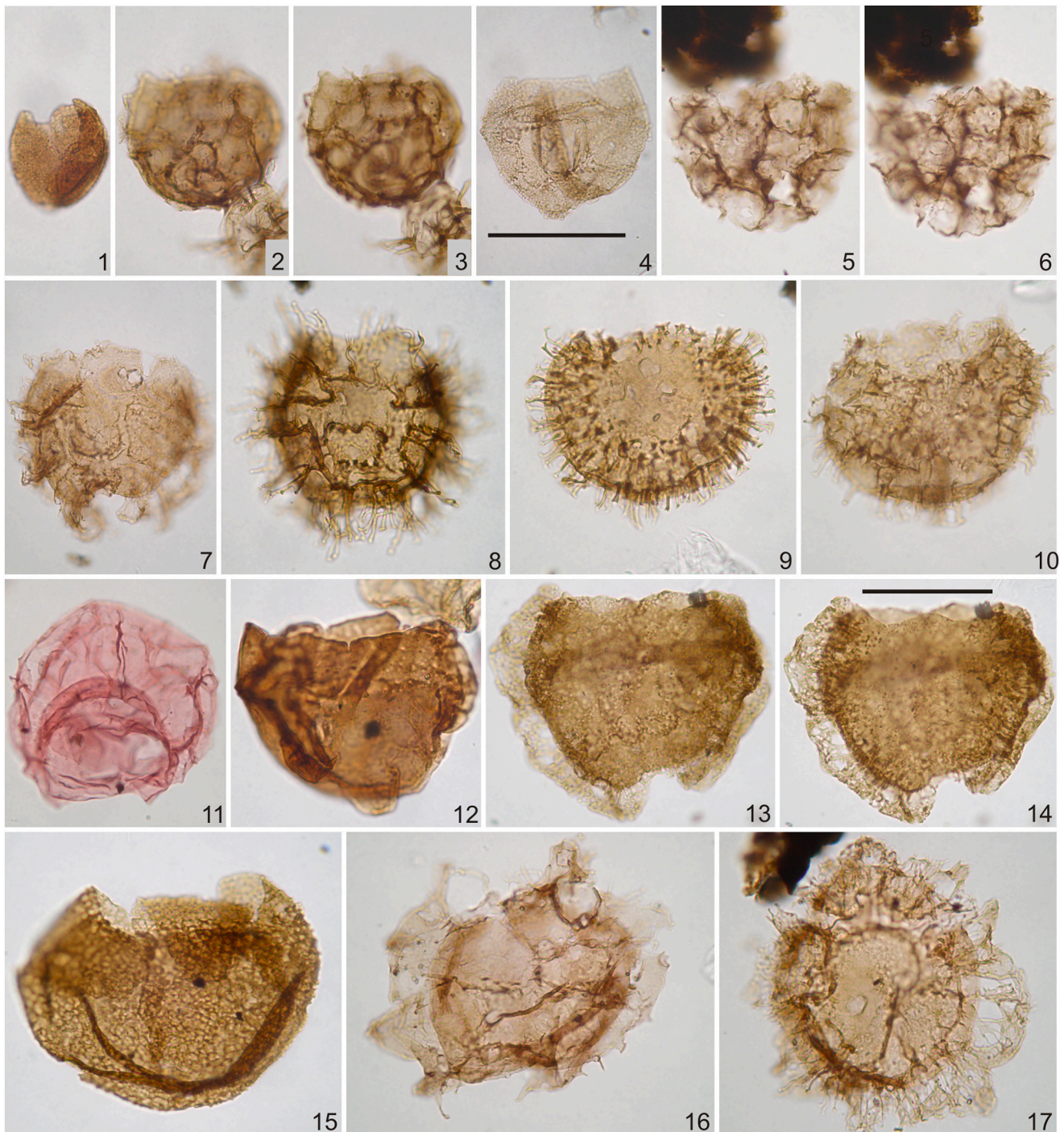
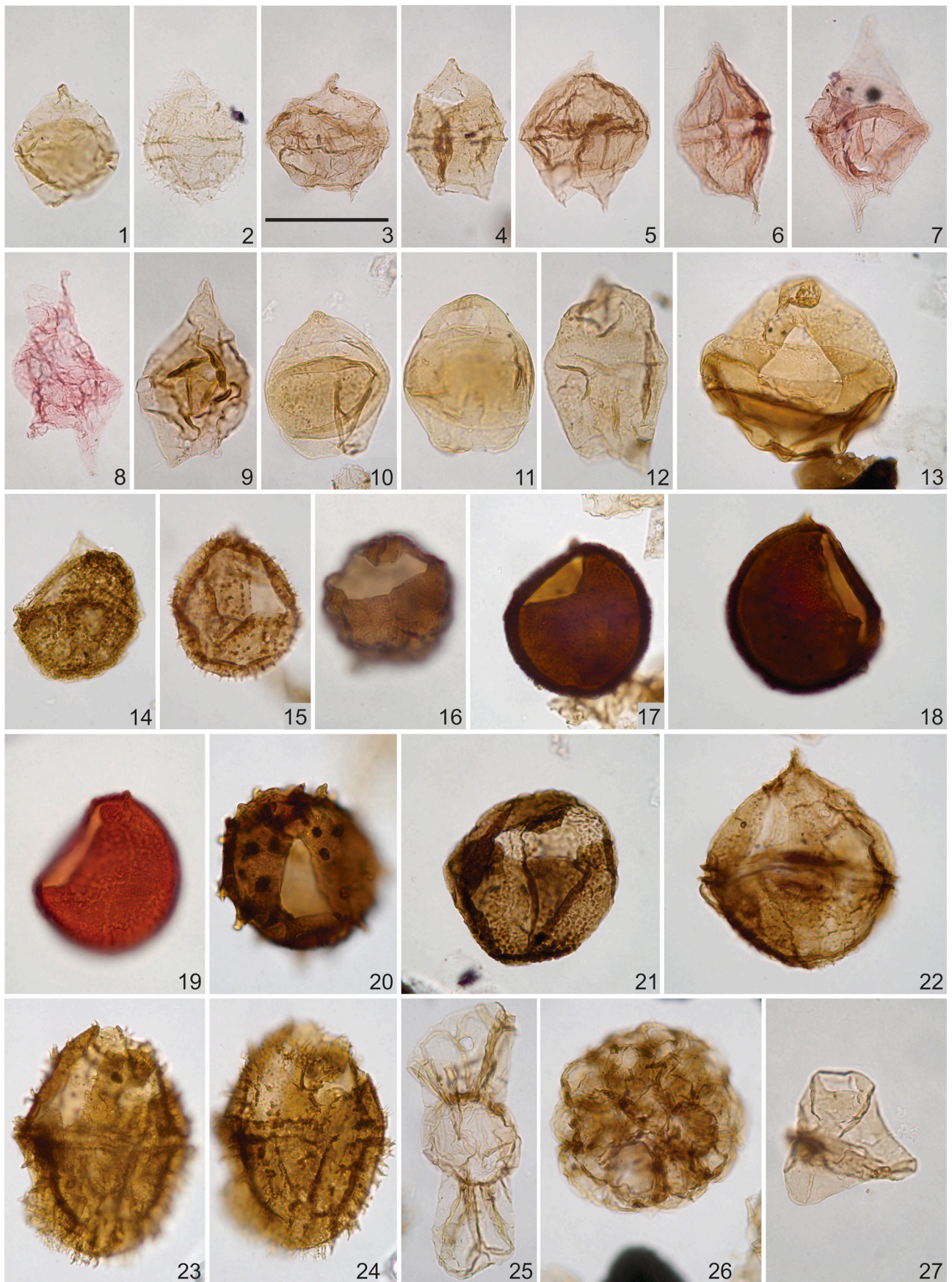


**Plate 2.** Campanian dinoflagellate cysts from the Bou Lila outcrop, western External Rif, northwestern Morocco. Scale bars represents 40  $\mu\text{m}$ .

1. *Batiacasphaera solida*; sample KBL14, slide 1, EF O27.
- 2, 3. *Valensiella foucheri*; sample KBL11, slide 2, EF H36/2.
4. *Canninginopsis bretonica*; sample KBL15, slide 1, EF X39; dorsal surface.
- 5, 6. *Cyclonephelium filoreticulatum?*; sample KBL11, slide 2, EF C47/3.
7. *Areoligera coronata*; sample KBL5, slide 2, EF V27/2; dorsal surface.
8. *Areoligera senonensis*; sample KBL13, slide 2, EF H45; dorsal surface.
9. *Circulodinium distinctum* subsp. *distinctum*; sample KBL7, slide 2, EF S60;
10. *Heterosphaeridium heteracanthum* subsp. *heteracanthum*; sample KBL14, slide 1, EF R43/3; focus on the apical archeopyle and processes.
11. *Turnhosphaera hypoflata*; sample KBL4, slide 2, EF L56/2.
12. *Senoniasphaera rotundata*; sample KBL8, slide 2, EF W39/1; dorsal surface.
- 13, 14. *Senoniasphaera reticulata* in [Wilson \(1974\)](#); sample KBL13, slide 1, EF S44/4; dorsal surface (13), ventral surface (14).
15. *Cassiculosphaeridia? intermedia*; sample KBL10, slide 2, EF Q24/2; focus on the wall structure and archeopyle.
16. *Palynodinium gallator*; sample KBL13, slide 1, EF C28/1; dorsal surface.
17. *Glaphyrocysta wilsonii*; sample KBL6, slide 2, EF J31/3; dorsal surface.





(caption on next page)



**Plate 3.** Campanian dinoflagellate cysts from the Bou Lila outcrop, western External Rif, northwestern Morocco. Scale bars represents 40  $\mu\text{m}$ .

1. *Alterbidinium varium*; sample KBL12, slide 2, EF C24/2; dorsal surface.
2. *Palaeohystrichophora infusorioides*; sample KBL5, slide 2, EF N26; dorsal surface.
3. *Senegalinium bicavatum*; sample KBL5, slide 2, EF R32/4; dorsal surface.
4. *Chatangiella madura*; sample KBL6, slide 2, EF H33/1; dorsal surface.
5. *Cerodinium boloniense*; sample KBL5, slide 2, EF S36/6; dorsal surface. tripartite.
6. *Alterbidinium kirschii*; sample KBL2, slide 1, EF O49; dorsal surface.
7. *Chatangiella? robusta*; sample KBL2, slide 1, EF T32/3; dorsal surface with focus on the cingulum.
8. *Cerodinium diebelii*; sample KBL4, slide 2, EF G36.
9. *Alterbidinium acutulum*; sample KBL2, slide 1, EF A6/4.
10. *Isabelidinium variable*; sample KBL2, slide 2, EF 37/4; focus on the dorsal surface and intercalary type I (2a) archeopyle.
11. *Isabelidinium cretaceum*; sample KBL15, slide 1, EF A39; focus on the dorsal surface and intercalary type I (2a) archeopyle.
12. *Isabelidinium cooksoniae*; sample KBL13, slide 1, EF H26;
13. *Nelsoniella aceras*; sample KBL8, slide 2, EF N29/2; focus on the dorsal surface and intercalary type I (2a) archeopyle.
14. *Apteodinium deflandrei*; sample KBL13, slide 2, EF R45; focus on the precingular type P(3'') archeopyle.
15. *Trichodinium castanea* subsp. *castanea*; sample KBL15, slide 1, EF Z44; focus on the precingular type P(3'') archeopyle.
16. *Trithyrodinium evittii*; sample KBL14, slide 1, EF V50/3; focus on the dorsal surface and intercalary type 3I archeopyle.
17. *Apteodinium crassum*; sample KBL14, slide 1, EF W47; focus on the thick wall and precingular type P(3'') archeopyle.
18. *Apteodinium crassum*; sample KBL14, slide 1, EF H29/4; focus on the thick wall and precingular type P(3'') archeopyle.
19. *Cribroperidinium graemei*; sample KBL2, slide 1, EF G48/2; focus on the tabulated wall and precingular type P(3'') archeopyle.
20. *Exochosphaeridium brevitrunctum*; sample KBL10, slide 2, EF F43/3; Dorsal surface.
21. *Trithyrodinium suspectum*; sample KBL11, slide 2, EF Q51; focus on the dorsal surface and intercalary type 3I archeopyle.
22. *Cribroperidinium cooksoniae*; sample KBL5, slide 2, EF F30/4; dorsal surface.
- 23, 24. *Cribroperidinium wilsonii* subsp. *wilsonii*; sample KBL12, slide 2, EF N40/4; dorsal surface (23), ventral surface (24).
25. *Codoniella campanulata*; sample KBL14, slide 1, EFJ48/2.
26. *Palambage* sp.; sample KBL7, slide 2, EF D46.
27. *Trigonopyxidia ginella*; sample KBL7, slide 2, EF U36.

Crimea (Guzhikov et al., 2020). The Campanian dinoflagellate cyst assemblages, recorded in the Maastricht region and northern Belgium, including most of the new dinoflagellate cyst taxa described by Slimani (1994, 1996, 2001b, 2003), were later encountered in the Global Stratotype Section and Point GSSP for the base of the Maastrichtian (Tercis les Bains, Landes, SW France) (Antonescu et al., 2001a, 2001b; Schiøler and Wilson, 2001). They helped to separate the Campanian strata from of those assigned to the Maastrichtian age during a multidisciplinary study carried out in this French region and to make biostratigraphic correlations with several boreal and Tethyan Campanian successions. Among these dinoflagellate cysts, the following species (with Wilson's (1974) unpublished synonyms in brackets) are considered to be relevant by their first or last appearance datums for the determination of the Campanian in the Bou Lila section (this paper):

Species with relevant first appearance datums are: *Areoligera coronata*, *Areoligera senonensis*, *Batiacasphaera solida* (*Chytroisphaeridia solida*), *Cassiculosphaeridia? intermedia* (*Chytroisphaeridia everricula*), *Cerodinium diebelii*, *Chatangiella? robusta* (*Trithyrodinium inaequale*), *Cribroperidinium graemei* (*Cribroperidinium filosum*), *Glapyrocysta wilsonii* (*Glapyrocysta perforatum*), *Impagidinium rigidaseptatum* (*Spiniferites cingulatus* var. *prominoseptatus*), *Nematosphaeropsis philippotii* (*Nematosphaeropsis delicata*), *Palynodinium grillator*, *Rigaudella appenninica* (*Adnatosphaeridium* cf. *aemulum*), *Rottnestia wetzeli* subsp. *brevispinosa* (*Hystrichosphaeropsis jubata*), *Senoniasphaera reticulata* in Wilson (1974), *Trithyrodinium evittii* and *Turnhosphaera hypoflata* (*Nelsoniella glomerata*);

Species with relevant last appearance datums are: *Cribroperidinium wilsonii* subsp. *wilsonii* (*Acanthaulax saetosa*), *Odontochitina costata*, *Odontochitina operculata* and *Xenascus ceratioides*;

Species with relevant first and last appearance datums are: *Raetiaedinium belgium*, *Senoniasphaera alveolata* in Wilson (1974) and *Xenascus wetzeli* (*Odontochitina wetzeli*).

Most of these synonyms are given in Slimani (1994, 1995) and Slimani (2001a), pp. 192–194.

Dinoflagellate cyst assemblages, mostly similar to those of the Maastricht region and northern Belgium, were also recorded in Campanian strata from Hornby Island, British Columbia, Canada (McLachlan et al., 2018). Other Campanian dinoflagellate cyst assemblages were studied in the east coast region of the United States of America (Aurisano and Habib, 1977; May, 1980; Aurisano, 1989; Habib and Miller, 1989),

Canada and Greenland (McIntyre, 1975; Ioannides, 1986; Williams et al., 2004; Fensome et al., 2009, 2016), England (Costa and Davey, 1992), Norway (Setoyama et al., 2013), Siberia (Lebedeva et al., 2017) and Sambian Peninsula (Aleksandrova and Zaporozhets, 2008).

In the Mediterranean regions, several studies were undertaken on Campanian dinoflagellate cyst assemblages from Spain (Riegel Riegel, 1974; Riegel and Sarjeant, 1982; Radmacher et al., 2014), Italy (Corradini, 1973; Roncaglia and Corradini, 1997; Roncaglia, 2002), Austria (Skupien and Mohamed, 2008; Mohamed and Wagreich, 2013), Middle East (Eshet et al., 1994; Hoek et al., 1996) and Egypt (Schrank, 1987; El Beialy, 1995; Schrank and Ibrahim, 1995; Makled et al., 2014). Campanian dinoflagellate cyst assemblages were also studied in other regions of North Africa from Ivory Coast (Masure et al., 1998), Ghana (Atta-Peters and Salami, 2004), Gulf of Guinea (Sánchez-Pellicer et al., 2017) and elsewhere (Stover et al., 1996; Williams et al., 1993, 2004).

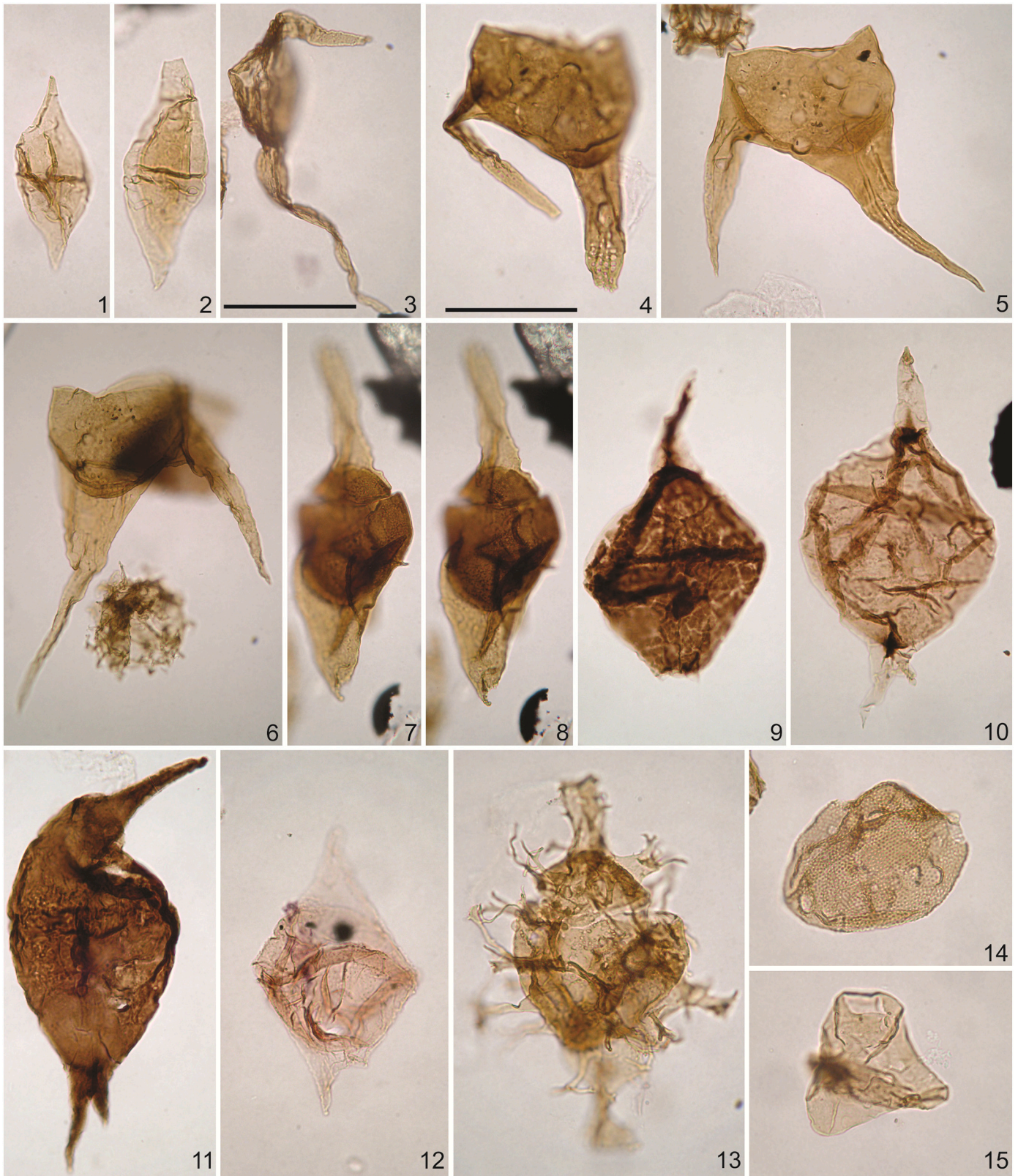
In Morocco, the most important palynological studies, dealing with systematics, biostratigraphy and paleoenvironment of Campanian dinoflagellate cysts, were carried out in the "Phosphate Plateau" (Soncini and Rauscher, 1988; Soncini, 1990) and in the Rif Chain, in the Sekada section (Guédé, 2016; Slimani et al., 2016) and Tattofte section (Jbari et al., 2020). The Sekada and Tattofte sections are located at ~40 km northeast and ~6 km south of the studied section, respectively.

## 5. Results

All the analyzed samples are very productive and the palynomorphs are well preserved. The identified assemblage is abundant in marine palynomorphs, particularly in dinoflagellate cysts (91%), associated with rare occurrences of algae (e.g., *Palambages*: 4%), acritarchs (2%), microfossiliferous test linings (1%) and spores and pollen grains (2%) (Fig. 4). All the dinoflagellate cyst taxa observed are listed in an order of their first occurrences in Table 1 and in an alphabetical order in Appendix A.

Among the marine palynomorphs, 79 dinoflagellate cyst species have been recorded, including more than 40 taxa, which are good biostratigraphic markers of the late Campanian (Table 1). These include *Andalusiella gabonnensis*, *Andalusiella ivoiriensis*, *Andalusiella mauthei* subsp. *mauthei*, *Andalusiella mauthei* subsp. *punctata*, *Andalusiella spicata*, *Areoligera coranata*, *Areoligera flandriensis*, *Areoligera senonensis*,





(caption on next page)



**Plate 4.** Campanian dinoflagellate cysts from the Bou Lila outcrop, western External Rif, northwestern Morocco. Scale bars represents 40  $\mu\text{m}$ .

1. *Biconidinium reductum*; sample KBL6, slide 2, EF S32/3.
2. *Biconidinium reductum*; sample KBL5, slide 2, EF Q36.
3. *Palaeocystodinium lidiae*; sample KBL11, slide 2, EF U50/1.
4. *Odontochitina porifera*; sample KBL13, slide 2, EF J43/3.
5. *Odontochitina costata*; sample KBL12, slide 3, EF V37/2.
6. *Odontochitina operculata*; sample KBL12, slide 2, EF K53/3.
7. 8. *Xenascus wetzeli*; sample KBL7, slide 2, EF G46.
9. *Andalusiella ivoirensis*; sample KBL5, slide 2, EF S49.
10. *Andalusiella spicata*; sample KBL5, slide 2, EF M31.
11. *Andalusiella mauthei* subsp. *mauthei*; sample KBL5, slide 2, EF C37/3.
12. *Chatangiella? robusta*; sample KBL2, slide 1, EF T32/3; focus on the tripartite cingulum.
13. *Xenascus ceratioides*; sample KBL10, slide 2, EF G38/2.
14. *Rigaudella appenninica*; sample KBL14, slide 1, EF V50/4.

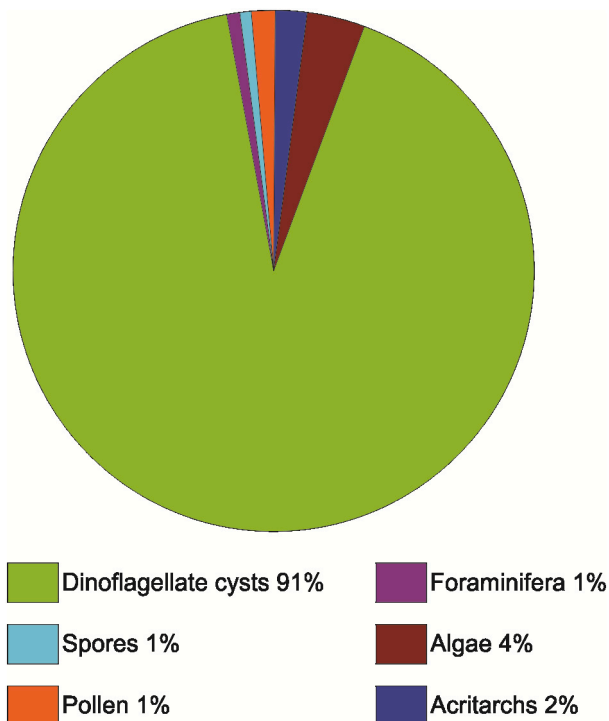


**Fig. 4.** Percentage of the main groups of palynomorphs (dinoflagellate cysts, sporomorphs, acritarchs, algae, foraminifera) in the Bou Lila section, region of Ksar El-Kébir, western External Rif, northwestern Morocco.

*Chatangiella? robusta*, *Cassiculosphaeridia? intermedia*, *Criboperidinium wilsonii* subsp. *wilsonii*, *Impagidinium rigidaseptatum*, *Nelsoniella aceras*, *Nematosphaeropsis philippotii*, *Odontochitina costata*, *Odontochitina operculata*, *Odontochitina porifera*, *Palynodinium grallator*, *Raetiaedinium belgicum*, *Rigaudella appenninica*, *Rottnestia wetzeli* subsp. *brevispinosa*, *Senegalinium bicavatatum*, *Trichodinium castanea* subsp. *castanea*, *Trigonopyxidiella ginella*, *Xenascus ceratioides* and *Xenascus wetzeli*.

From a quantitative point of view, the dinoflagellate cyst groups, which record significant changes in their relative abundance along the Bou Lila section, include 6 groups of gonyaulacoid taxa and 2 groups of peridinoid taxa, previously considered as paleoenvironmental indicators (Tables 2, 3). These dinoflagellate cyst groups, followed by the included dinoflagellate cyst taxa between brackets, are: *Areoligera-Glaphyrocysta* (*Areoligera*, *Glaphyrocysta*), *Deflandrea* (*Alterbidinium*, *Cerodinium*, *Isabelidinium*, *Lejeunecysta*, *Phelodinium*, *Senegalinium*, *Spinidinium*), *Cordosphaeridium* (*Fibrocysta*, *Cordosphaeridium*, *Operculodinium*), *Spiniferite-Achomosphaera* (*Spiniferites*, *Achomosphaera*), *Cleistosphaeridium*, *Impagidinium* (*Impagidinium*, *Pterodinium*), *Odontochitina* and *Palaeohystrichophora* (Fig. 6). The *Andalusiella*, *Cordosphaeridium*, *Deflandrea*, *Spiniferites-Achomosphaera* and *Palaeohystrichophora* groups

are the most abundant, reaching a maximum of 45%, 50%, 20%, 35% and 35%, respectively. The other groups (*Areoligera-Glaphyrocysta*, *Cleistosphaeridium*, *Impagidinium*, *Odontochitina*) record lower relative abundances ( $\leq 10\%$ ). The relative abundance of the *Andalusiella* group is maximum at the base of the section (45% in sample KBL1), but decreases towards the top, whereas that of the *Spiniferites-Achomosphaera* and *Cordosphaeridium* groups is minimum (5%, 8%) at the base, but increase upwards to a maximum of 50%, 38%, respectively (Table 3, Fig. 6). S/D ratios are very low (0–0.025). They are generally higher in the yellowish marls. P/G and IN/ON ratios vary between 0.1 and 0.8, with a maximum at the base of the section in samples KBL1 and KBL2, and gradually decrease upwards. The results of the counted particles of the three main groups of kerogen (Phytoclasts, AOM, Palynomorphs) are plotted in an AOM–Phytoclasts–Palynomorphs ternary diagram after Tyson (1995) (Fig. 7) and in Figure 8. The results show that most of the samples analyzed are characterized by a dominance of palynomorphs (essentially dinoflagellate cysts: 55–80%) and phytoclasts (20–45%). However, all samples contain a small amount of amorphous organic matter (3–12%). The lowermost part of the section (samples KBL1, KBL2) contains mainly phytoclasts (mostly coaly opaque fragments, belonging to the inertinite group: 58–60%), while the uppermost part (samples KBL14, KBL15) is the richest in palynomorphs (mostly dinoflagellate cysts: 75–80%). Spores and pollen grains are very rare (0.7%).

The calcium carbonate content ( $\text{CaCO}_3$ ) is moderate throughout the section (20–35%).

## 6. Interpretations

### 6.1. Age determinations

The Bou Lila section is dated as late Campanian based on marker bioevents (FADs and LADs) of selected dinoflagellate cyst species, whose stratigraphic distributions are plotted in Table 1. The biostratigraphic interpretations are based mainly on comparisons with Campanian dinoflagellate cyst assemblages from biostratigraphically well-calibrated sequences, including those of the Campanian type area in Charente (Neumann et al., 1983), in the GSSP for the base of the Maastrichtian in Tercis les Bains (Antonescu et al., 2001a, 2001b; Schiøler and Wilson, 2001) and in the Maastrichtian type area in Limbourg (Wilson, 1974; Foucher, 1985; Slimani, 1994, 1995, 2001a, 2003; Slimani and Louwey, 2013). Comparisons were also helpful with dinoflagellate cyst assemblages from northern Belgium (Slimani, 1994, 1995, 1996, 2000, 2001a, 2001b, 2003; Slimani et al., 2011; Slimani and Louwey, 2013), England (Costa and Davey, 1992), Denmark (Wilson, 1971, 1974; Surlyk et al., 2013) and other regions from North Europe, USA, Canada and Greenland. Dinoflagellate cyst assemblages from the Mediterranean regions, such as Italy (Corradini, 1973; Roncaglia and Corradini, 1997; Roncaglia, 2002), Spain (Radmacher et al., 2014), Morocco (Soncini and Rauscher, 1988; Soncini, 1990; Slimani et al., 2010, 2016; Jbari et al., 2020), North Africa and from elsewhere (Stover et al., 1996; Williams et al., 2004) were very useful for this study

**Table 1**  
 Ranges of stratigraphically significant dinoflagellate cyst species from the upper Campanian marly succession in the Bou Lila section, western External Rif, northwestern Morocco.

SERIES		LITHOLOGY	Species	
STAGE				
Samples				
Upper Cretaceous	Upper Campanian	Grey marls	KBL15	
			KBL14	
			KBL13	
			KBL12	
		Yellowish-grey marls	KBL11	
			KBL10	
			KBL9	
			KBL8	
			KBL7	
			KBL6	
		Yellowish marls	KBL5	
			KBL4	
			KBL3	
			KBL2	
			KBL1	
			1	<i>Andalusella spicata</i>
			2	<i>Nelsonella aceras</i>
			3	<i>Trifaridium suspectum</i>
			4	<i>Senoniasphaera protrusa</i>
			5	<i>Aplecodinium deflandrei</i>
			6	<i>Alterbidinium acutulum</i>
			7	<i>Alterbidinium minus</i>
			8	<i>Alterbidinium varium</i>
			9	<i>Biconodinium reductum</i>
			10	<i>Circulodinium distinctum</i> subsp. <i>distinctum</i>
			11	<i>Coronifera oceanica</i>
			12	<i>Citroparidinium graemei</i>
			13	<i>Dinogymnium digitus</i>
			14	<i>Elytrocysta drugii</i>
			15	<i>Isabelidinium cretaceum</i>
			16	<i>Isabelidinium variabile</i>
			17	<i>Odonotochitina costata</i>
			18	<i>Palaeohystrichophora infusorioides</i>
			19	<i>Pterodinium cretaceum</i>
			20	<i>Trichodinium castanea</i> subsp. <i>castanea</i>
			21	<i>Turniosphaera hypoflata</i>
			22	<i>Alterbidinium kirchii</i>
			23	<i>Andalusella gabonensis</i>
			24	<i>Andalusella mauthei</i> subsp. <i>punctata</i>
			25	<i>Cerodinium boloniense</i>
			26	<i>Cerodinium leptodermum</i>
			27	<i>Odonotochitina porifera</i>
			28	<i>Chatangiella? robusta</i>
			29	<i>Odonotochitina operculata</i>
			30	<i>Cyclonophellium filoreticulatum?</i>
			31	<i>Citroparidinium cooksoniae</i>
			32	<i>Impagidinium cristatum</i>
			33	<i>Trifaridium evitii</i>
			34	<i>Andalusella ivorensis</i>
			35	<i>Senegalium bicavatum</i>
			36	<i>Sarculosphaeridium longifurcatum</i>
			37	<i>Andalusella mauthei</i> subsp. <i>mauthei</i>
			38	<i>Citroparidinium wilsonii</i> subsp. <i>wilsonii</i>
			39	<i>Isabelidinium cooksoniae</i>
			40	<i>Raetaedinium belgicum</i>
			41	<i>Rothensta wetzelii</i> subsp. <i>brevispinosa</i>
			42	<i>Senoniasphaera rotundata</i>
			43	<i>Codonella campanulata</i>
			44	<i>Canningiopsis bretonica</i>
			45	<i>Cannosphaeropsis ulmensis</i>
			46	<i>Cassiculosphaeridia? intermedia</i>
			47	<i>Cerodinium diebelli</i>
			48	<i>Florentinia aculeata</i>
			49	<i>Florentinia ferax</i>
			50	<i>Xenascus wetzelii</i>
			51	<i>Glaphrocysta wilsonii</i>
			52	<i>Phelodinium magnificum</i>
			53	<i>Areoligera coronata</i>
			54	<i>Areoligera senonensis</i>
			55	<i>Senoniasphaera reticulata</i> in Wilson (1974)
			56	<i>Areoligera fiandriensis</i>
			57	<i>Nematospaeropsis philippotii</i>
			58	<i>Nematospaeropsis cf. latiflata</i> Wrenn, 1988.
			59	<i>Unipontidinium grande</i>
			60	<i>Xenascus ceratoides</i>
			61	<i>Chatangiella madura</i>
			62	<i>Impagidinium</i> sp. of Simani et al. (2016)
			63	<i>Raetaedinium laevigatum</i>
			64	<i>Senoniasphaera alveolata</i> in Wilson (1974)
	65	<i>Rigaudella apenninica</i>		
	66	<i>Polynodinium grallator</i>		
	67	<i>Tanyosphaeridium xanthiopyxides</i>		
	68	<i>Hystriodinium puchrum</i>		
	69	<i>Exochosphaeridium brevitrunceum</i>		
	70	<i>Trigonopyxidia ginella</i>		
	71	<i>Chatangiella dilissima</i>		
	72	<i>Valensiaella rouchei</i>		
	73	<i>Palaeocystodinium lidiae</i>		
	74	<i>Diphyes colligerum</i>		
	75	<i>Impagidinium scrosum</i>		
	76	<i>Aplecodinium crassum</i>		
	77	<i>Batiacasphaera solida</i>		
	78	<i>Heterosphaeridium heteracanthum</i> subsp. <i>heteracanthum</i>		
	79	<i>Impagidinium rigidaseptatum</i>		

Ranges of stratigraphically most significant dinoflagellate cyst species are shaded in grey.

**Table 2**  
Paleoenvironmental interpretations of selected dinoflagellate cyst groups, after references.

Dinocyst groups		Dinocyst taxa	Paleoenvironments	References
Gonyaulacooids	Peridinoids			
<i>Areoligera</i> - <i>Glaphyrocysta</i>		<i>Areoligera</i> , <i>Glaphyrocysta</i>	Shallow open marine inner neritic environments, close to the coast with a high energy and increased water stratification. It may indicate, in great abundance, a marine transgression.	Brinkhuis et al. (1992), Brinkhuis (1994), Powell et al. (1996), Stover et al. (1996)
<i>Spiniferites</i> - <i>Achomosphaera</i>		<i>Achomosphaera</i> , <i>Spiniferites</i>	Outer neritic to oceanic environments with stable salinity. Cosmopolitan and can be associated with upwellings and river discharges.	Wall et al. (1977), Brinkhuis (1994), Stover et al. (1996).
<i>Cordosphaeridium</i>		<i>Cordosphaeridium</i> , <i>Fibrocysta</i> , <i>Operculodinium</i>	Open neritic environments, associated with transgression.	Brinkhuis (1994), Powell et al. (1996), Sluijs et al. (2005).
<i>Impagidinium</i>		<i>Impagidinium</i> , <i>Pterodinium</i>	Oceanic to outer neritic oligotrophic environments	Brinkhuis (1994), Powell et al. (1996), Pross and Brinkhuis (2005)
<i>Cleistosphaeridium</i> <i>Odontochitina</i>		<i>Cleistosphaeridium</i> <i>Odontochitina</i>	Outer neritic. Outer neritic environments.	Sluijs et al. (2005). Wilpshaar and Leereveld (1994), Leereveld (1995)
	<i>Andalusiella</i>	<i>Andalusiella</i> , <i>Palaeocystodinium</i>	Tropical-subtropical, nearshore environment with a rich nutrient availability. This group tolerates and thrive in high productivity upwelling systems.	Wall et al. (1977), Lentin and Williams (1980), Brinkhuis et al. (1998)
	<i>Deflandrea</i>	<i>Alterbidinium</i> , <i>Cerodinium</i> , <i>Isabelidinium</i> , <i>Lejeunecysta</i> , <i>Phelodinium</i> , <i>Senegalinium</i> , <i>Spinidinium</i>	Coastal and inner neritic environments with high nutrients and high productivity.	Brinkhuis et al. (1992), Brinkhuis (1994), Stover et al. (1996)
	<i>Palaeohystrichophora</i>	<i>Palaeohystrichophora</i>	Inner neritic environments with high nutrients, high productivity to outer neritic and also upwelling conditions.	Habib and Miller (1989), Pearce et al. (2009), Peyrot et al. (2011), Prauss (2012)

(refer back to chapter 4: previous studies on Campanian dinoflagellate cyst assemblages).

The biostratigraphic interpretations of the studied section are given from oldest to youngest as follows:

The following species, whose FADs are known in the Campanian (early–late Campanian) are *Andalusiella gabonensis*, *Andalusiella ivoiriensis*, *Andalusiella spicata*, *Andalusiella mauthei* subsp. *mauthei*, *Andalusiella mauthei* subsp. *punctata* (May, 1980; Schrank, 1987; Soncini, 1990; Williams et al., 1993; Schrank and Ibrahim, 1995; Hoek et al., 1996; Masure et al., 1998; Slimani et al., 2016; Sánchez-Pellicer et al., 2017; Jbari et al., 2020) and *Biconidinium reductum* (May, 1980; Kirsch, 1991; Slimani, 1995; Antonescu et al., 2001a, 2001b; Schiøler and Wilson, 2001; Slimani, 2001a). The FAD of *Alterbidinium varium* was recorded in late Campanian strata in the Mediterranean and southern Europe (Eshet et al., 1994; Hoek et al., 1996; Antonescu et al., 2001a, 2001b; Schiøler and Wilson, 2001; Slimani et al., 2016; Jbari et al., 2020), or at the Campanian–Maastrichtian boundary in northern Europe (Kirsch, 1991; Slimani, 2000, 2001a; Slimani et al., 2011; Surlyk et al., 2013). The FAD of *Alterbidinium kirschii* was also reported in the late Campanian in Morocco (Jbari et al., 2020), or in the early Maastrichtian in Europe (Kirsch, 1991 as *Alterbidinium* sp. A; Slimani, 1994, 1995, 2000, 2001a). *Pterodinium cretaceum* ranges from the late Campanian to the Cretaceous–Paleogene boundary (Schiøler and Wilson, 1993; Slimani, 1995, 2000, 2001a; Roncaglia and Corradini, 1997; Torricelli and Amore, 2003; Slimani et al., 2008, 2010, 2016; Guédé et al., 2014; Jbari et al., 2020) (see Slimani et al., 2010, p. 104). In the Bou Lila section, the previous *Andalusiella* species first occur successively within the sample interval KBL1–KBL3 (lower part of the section). *Alterbidinium varium*, *Biconidinium reductum* and *Pterodinium cretaceum* first occur in sample KBL1 and *Alterbidinium kirschii* first occurs in sample KBL2.

The FAD of *Chatangiella? robusta* is a potential marker of the late Campanian in the Northern Hemisphere (Wilson, 1974; Aurisano, 1989; Slimani, 1995; Hoek et al., 1996; Antonescu et al., 2001b; Schiøler and Wilson, 2001; Slimani, 2001a, Slimani and Louwye, 2011; Jbari et al., 2020). The FAD of *Trithyrodinium evittii* was reported in the late Campanian in southern Europe and Mediterranean regions (Antonescu et al., 2001a, 2001b; Schiøler and Wilson, 2001; Skupien and Mohamed, 2008; Slimani et al., 2016; Jbari et al., 2020), or at the

Campanian–Maastrichtian boundary in the Equatorial Realm (Williams et al., 2004), or in the early Maastrichtian in northern Europe (Slimani, 1995, 2000, 2001a; Kirsch, 1991; Marheinecke, 1992) and USA (May, 1980; Aurisano, 1989). In the northern and southern Hemisphere high latitudes the FAD of *Trithyrodinium evittii* is younger (uppermost Maastrichtian to Danian) than in the middle latitudes and equatorial regions (Wilson, 1984; Helby et al., 1987; Nøhr-Hansen and Dam, 1997; Brinkhuis et al., 1998; Williams et al., 2004; Vieira et al., 2018, 2020). The FAD of *Trithyrodinium evittii* is then indicative of late Campanian in the southern Europe and Mediterranean regions (including the studied section), and Maastrichtian to Danian elsewhere in the Southern and Northern Hemisphere. *Chatangiella? robusta* and *Trithyrodinium evittii* are associated with *Cerodinium leptodermum*, *Cerodinium boloniense* and *Senegalinium bicavatum*, whose FADs are also known in the late Campanian (Slimani, 1995, 2001a; Roncaglia and Corradini, 1997; Oboh-Ikuenobe et al., 1998; Torricelli and Amore, 2003; Williams et al., 2004; Slimani et al., 2016; Guédé et al., 2014; McLachlan et al., 2018; Jbari et al., 2020). In the Bou Lila section, *Senegalinium bicavatum* first occurs in sample KBL3 and the other species in sample KBL2.

*Raetiaedinium belgicum* and *Xenascus wetzeli*, which are restricted to the late Campanian, and *Canninginopsis bretonica* and *Cassiculosphaeridia? intermedia*, of which the FADs were also recorded in the late Campanian (Wilson, 1974; Foucher, 1985; Slimani, 1994, 1995, 1996, 2001a, 2001b, Antonescu et al., 2001b), first occur in the sampling interval KBL3–KBL4. The FAD of *Cerodinium diebelii*, which is a worldwide marker of the late Campanian (Antonescu et al., 2001a, 2001b; Slimani, 2001a; Wilson and Schiøler, 2001; Williams et al., 2004; Radmacher et al., 2014; Slimani et al., 2016) is recorded in sample KBL4.

The FADs of *Areoligera coronata*, *Areoligera senonensis*, *Glaphyrocysta wilsonii*, *Rigaudella appenninica*, *Palynodinium gallator* and LADs of *Cribroperidinium wilsonii* subsp. *wilsonii* and *Chatangiella madura* are good markers of the late Campanian in the Northern Hemisphere (Wilson, 1974; Foucher, 1985; Kirsch, 1991; Roncaglia and Corradini, 1997; Costa and Davey, 1992; Slimani, 1995, 2000, 2001a; Williams et al., 2004; Antonescu et al., 2001a, 2001b; Wilson and Schiøler, 2001; Surlyk et al., 2013; Radmacher et al., 2014; Slimani et al., 2011, 2016; McLachlan et al., 2018; Jbari et al., 2020). In this study, these species are present in the upper part of the section (samples KBL5 to KBL15). They



**Table 3**  
Quantitative palynological data from the upper Campanian marly succession in the Bou Lila section, region of Ksar El-Kébir, western External Rif, northwestern Morocco.

System	Series	Stage	Lithology	Dinoflagellate cyst groups (%)										Total Gonyaul = acoides (G)	Total P/G = NP+ ellate (D)	Total Spores (S)	S/D = nS+ nD	Total dino flag ellate cysts (IN)	IN/ON = nN/ +nON	Palynofacies (%)							
				Areoligera- Glaphy rocysta	Cordos phaert dium	Palaeo hystri cho phaera	Cleisto sphaeridium	Odon to chitina	Spinife ritina	Impagi dinium	Andal usiella	Deflan drea	Peridi noids (P)							Amor phous (AOM)	Organic Matter	Paly nomor phas	Phyto clasts				
GRETA CEOUS	Upper Cretaceous	Grey marls	KBL15	21.7	4.21	26.3	31.8	4.74	2.89	16.6	0	8.68	4.74	172	208	0.45	122	2	2	0.02	113	70	0.49	4.2	73.2	22	
			KBL14	23.5	7.59	34.4	11.9	2.98	3.52	24.1	1.08	4.07	11.1	102	272	272	0.27	124	2	4	0.03	148	104	0.59	3.6	78.6	17.8
			KBL13	23.2	8.82	24.1	19.5	3.21	3.74	25.4	1.34	12	2.14	127	249	249	0.34	123	1	3	0.02	109	115	0.5	5.6	55.4	38.6
	Yellowish-grey marls	KBL12	34.7	17	27.5	7.93	3.97	7.08	27.5	0.57	2.55	4.82	61	295	295	0.17	134	5	5	0.04	130	130	0.56	11	61.4	26.6	
		KBL11	29	11.5	48.8	5.09	3.49	7.51	13.9	1.07	5.09	1.88	52	322	322	0.14	127	2	5	0.05	201	81	0.72	3.6	68.2	28.2	
		KBL10	37	15.2	20.6	16.9	0	7.04	25.4	3.1	4.23	7.04	107	253	253	0.3	136	2	2	0.01	107	128	0.47	6.4	62.4	31	
	Yellowish marls	KBL9	29.3	10.7	38.3	13.9	3.01	1.64	25.1	0.82	2.73	3.28	75	291	291	0.2	129	7	7	0.05	158	118	0.58	8.4	57	34	
		KBL8	31.7	6.68	23.3	20.6	0	2.41	28.9	2.67	6.15	7.49	137	239	239	0.36	130	3	6	0.04	103	133	0.45	3.2	61.4	34.8	
		KBL7	23.7	3.13	25.3	16.2	0	3.66	27.9	0.26	8.88	12	153	231	231	0.4	121	2	4	0.05	106	114	0.52	9.2	53	37.2	
	Yellowish marls	KBL6	11.8	19.5	28.9	0.57	0	2.55	37.7	3.68	3.4	2.83	27	326	326	0.08	111	4	6	0.08	140	178	0.56	12.2	49.6	37	
		KBL5	28	14.1	24.7	5.46	0	4.02	37.9	4.89	3.74	6.03	59	298	298	0.17	129	4	8	0.06	117	171	0.46	6.4	54.8	38.4	
		KBL4	32.4	7.78	9.28	22.8	0	4.49	29.9	3.59	8.68	16.5	175	184	184	0.49	135	3	3	0.02	57	119	0.36	8.8	45.4	45.8	
	Grey marls	KBL3	32.1	11.7	19.2	22	0	2.51	27.3	5.57	3.62	11.4	146	238	238	0.38	135	2	4	0.04	95	138	0.4	6	47.2	46.4	
		KBL2	22.4	6.91	6.08	25.1	0	0.83	16.6	5.25	24.6	14.1	234	129	129	0.64	122	3	8	0.08	47	83	0.52	5.6	43.6	50.2	
		KBL1	23.2	0	2.74	35.6	0	0	6.85	2.74	44.5	8.9	130	18	18	0.88	125	10	10	0.07	4	11	0.54	4.8	32.4	62.4	

are associated with *Apteodinium crassum*, *Areoligera flandriensis*, *Batiacaspheara solida*, *Exochosphaeridium brevitrunctum*, *Impagidinium rigidaseptatum*, *Impagidinium scabrosum*, *Nematosphaeropsis philippotii*, *Palaeocystodinium lidiae*, *Raetiaedinium laevigatum*, *Senoniasphaera alveolata* in Wilson (1974) and *Valensiella foucheri*. The latter species have also their FADs in the late Campanian in Europe (Wilson, 1974; Foucher, 1985; Slimani, 1994, 1995, 2001a; Antonescu et al., 2001a, 2001b; Schiøler and Wilson, 2001; Slimani et al., 2011; Slimani and Louwey, 2013; Surlyk et al., 2013) and Morocco (Slimani et al., 2016; Jbari et al., 2020).

In summary, all the above-cited dinoflagellate cyst species characterize the late Campanian in the Bou Lila section by their FADs or LADs. Furthermore, the following species, which occur worldwide in the late Campanian, but generally do not cross the Campanian–Maastriichtian boundary (Powell, 1992; Williams et al., 2004), are present in the Bou Lila section, confirming its late Campanian age: *Senoniasphaera rotundata*, *Surculosphaeridium longifurcatum*, *Odontochitina costata*, *Odontochitina operculata*, *Odontochitina porifera*, *Trigonopyxidina ginella*, *Trichodinium castanea* subsp. *castanea*, *Trithyrodinium suspectum* and *Xenascus ceratioides*. *Cyclonephelium floreticulatum?*, *Nelsoniella aceras* and *Senoniasphaera reticulata* in Wilson (1974), whose LADs are not younger than late Campanian (Wilson, 1974; Foucher, 1985; Helby et al., 1987; Louwey, 1991; Slimani, 1994, 1995, 2000, 2001a, 2003; Williams et al., 2004; Jbari et al., 2020), are present in the studied section and therefore support the suggested late Campanian age. The Campanian strata in the Bou Lila section are correlatable with two dinoflagellate cyst interval zones of Slimani (2001a); namely the *Exochosphaeridium? masureae* Zone (Subzone B: lower part of the late Campanian) based mainly on the first occurrences of *Biconidinium reductum*, *Raetiaedinium belgium* and *Xenascus wetzelii*, and the *Areoligera coronata* Zone (middle part of the late Campanian) based mainly on the first occurrences of *Areoligera coronata*, *Areoligera senonensis*, *Areoligera flandriensis*, *Palynodinium grillator* and *Rigaudella apenninica*. The top of the *Areoligera coronata* Zone is recognized based on the last occurrence of *Xenascus wetzelii* (Fig. 5). The *Hystrichokolpoma gamospina* Zone, defined between the two previous zones by Slimani (2001a), is not recognized in the study section, since the characteristic dinoflagellate cyst taxa of this zone are absent.

### 6.2. Paleocological interpretations of dinoflagellate cysts

The paleoenvironmental reconstructions inferred from dinoflagellate cysts are based on the following quantitative parameters: the relative abundances (%) of selected dinoflagellate cyst groups that are indicative of different paleoenvironments (Table 2) (refer back to chapter 5: results) and S/D, P/G and IN/ON ratios (Fig. 6). In the Bou Lila section, the *Andalusiella*, *Cordosphaeridium*, *Deflandrea*, *Spiniferites-Achomosphaera* and *Palaeohystrichophora* groups are the most abundant, however, the other groups (*Areoligera-Glaphyrocysta*, *Cleistosphaeridium*, *Impagidinium*, *Odontochitina*) are generally rare. The CaCO<sub>3</sub> content is moderate throughout the section (25–30%), but slightly higher in the middle part (mostly around 34% in the transition yellowish-grey marls) than in the rest of the section (around 25%). The fluctuations of the relative abundances of the dinoflagellate cyst groups, as well as, those of the P/G, S/D and IN/ON ratios, allowed the separation of three main paleocological Zones (A, B, C):

#### 6.2.1. Ecozone A (sampling interval KBL1–KBL4)

This ecozone extends from sample KBL1 to sample KBL4 (lower part of the section) and is correlated with the yellowish marls, dated herein as upper Campanian (lower part). The interval is characterized by the highest values of the S/D (up to 0.025), P/G (up to 0.9) and IN/ON (0.8) ratios and highest relative abundances of the following peridinioid dinoflagellate cyst groups: *Andalusiella* (up to 45%), *Deflandrea* (up to 20%) and *Palaeohystrichophora* (up to 35%). The gonyaulacoids are less abundant. They are mostly represented by the *Spiniferites-*

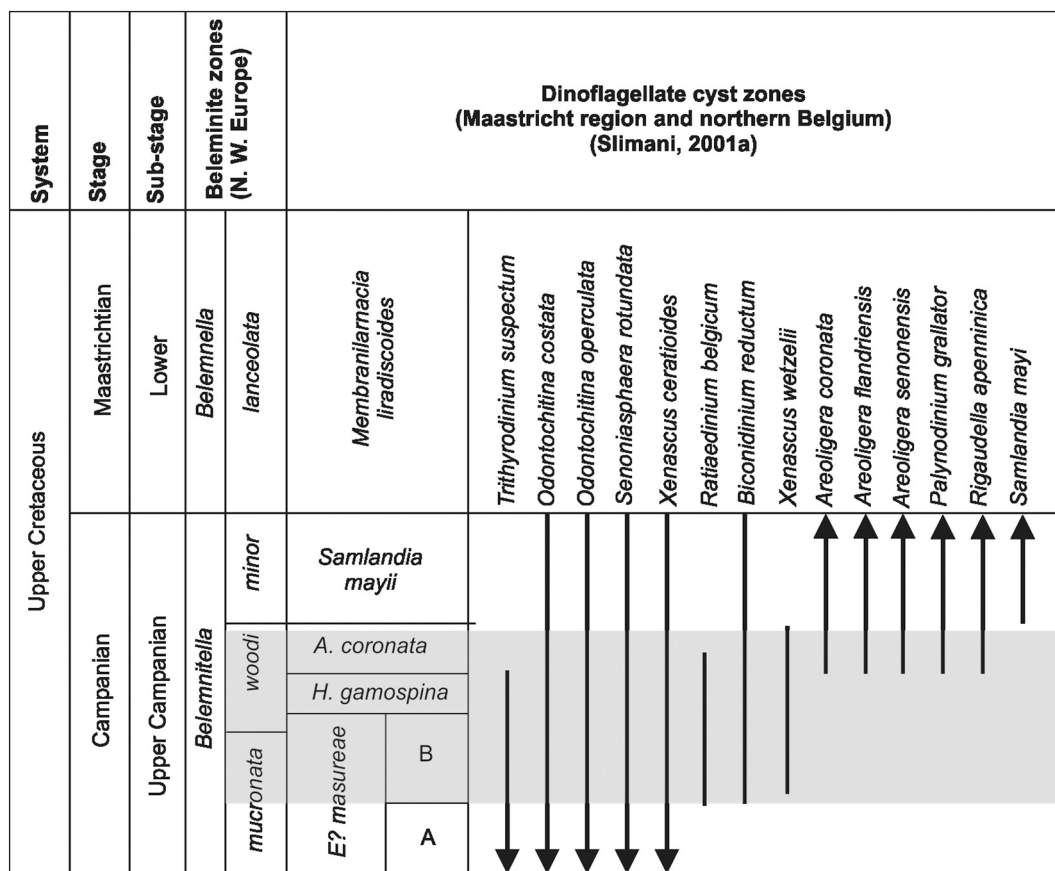


Fig. 5. Correlation of the Bou Lila section with the upper Campanian dinoflagellate cyst zones of Slimani (2001a), calibrated with North West Europe Belemnite zones (Ernst, 1964; Schulz, 1979; Christensen, 1995, 1999). The ranges of index dinoflagellate cyst species are also indicated. The highlighted (shaded in grey) area corresponds to the studied interval.

Achomosphaera group (up 30%); the Cordosphaeridium group is less abundant ( $\leq 10\%$ ) throughout this interval except for the sample KBL3 (20%). The other gonyaulacoid groups (Areoligera-Glyphyrocysta, Cleistosphaeridium, Impagidinium, Odontochitina) are rare (mostly 0–9%). In this ecozone (A), the relative abundances of the Andalusiella and Palaeohystrichophora groups record respectively a maximum of 45% and 35% in the most basal part of the section (sample KBL1), but decrease upwards to 23% and 25% in sample KBL2, 5% and 23% in sample KBL3 and 10% and 23% in sample KBL4. This decrease is associated with a gradual decrease of the P/G ratios (from 0.9 in sample KBL1 to 0.45 in sample KBL4). On the other hand, the relative abundances of the Spiniferites-Achomosphaera are inversely proportional to those of the Andalusiella and Palaeohystrichophora groups. The Andalusiella group proliferates in nearshore environment systems with warm-water marine conditions, a rich nutrient availability and a high productivity, typical of upwelling and a tropical to subtropical setting (Wall et al., 1977; Lentin and Williams, 1980; Brinkhuis et al., 1998). The Palaeohystrichophora group may also proliferate in shallower neritic environments with high nutrient input and also in upwelling conditions (Habib and Miller, 1989; Pearce et al., 2009; Prauss, 2012) as well as in outer neritic environments (Peyrot et al., 2011). The Spiniferite-Achomosphaera group is a cosmopolitan, being found in neritic and oceanic environments with stable salinity and low nutrient input, as well as in high-productivity zones, influenced by river flows and upwellings (Brinkhuis, 1994; Stover et al., 1996; Zonneveld et al., 2013). These findings on the dinoflagellate cyst groups and P/G ratios suggest for this ecozone (A): an inner to intermediate neritic setting reflecting ascending gradual offshore conditions, but with nearshore, warm-water and high productivity conditions in the most basal part of the section (samples KBL1,

KBL2), which may be related to an upwelling zone. The highest values of the IN/ON ratios, reaching  $\sim 0.8$  in sample KBL1 and  $\sim 0.7$  in sample KBL2, suggest lowest depths and therefore supports the suggested nearshore conditions for the most basal part of the section. In this interval, the Deflandrea group, which proliferates in shallower neritic with freshwater and high-productivity conditions (Brinkhuis et al., 1992; Brinkhuis, 1994; Stover et al., 1996), records moderate abundances (10–20%) and therefore supports the paleoenvironment inferred for this ecozone (A). The S/D ratios are proportional with the relative abundances of the Deflandrea group, confirming a nutrient supply of continental origin and freshwater conditions, favorable for the proliferation of the Deflandrea group in this ecozone (A). The presence of rare specimens assigned to the oceanic Impagidinium group in this marine neritic setting may likely be associated with the upwelling currents.

### 6.2.2. Ecozone B (sampling interval KBL5–KBL12)

This ecozone is correlated with the transition yellowish-grey marls, dated here as upper Campanian (middle to upper part). Compared to the previous ecozone (A), this ecozone records a significant increase in the relative abundances of the gonyaulacoid groups, mainly Spiniferites-Achomosphaera (up to 40%) and Cordosphaeridium (up to 50%). The Cordosphaeridium group, also proliferates in open neritic environments, but is associated with transgression (Brinkhuis, 1994; Powell et al., 1996; Sluijs et al., 2005). The other gonyaulacoid groups (Areoligera-Glyphyrocysta, Odontochitina, Impagidinium, Cleistosphaeridium) are rare, but record a slight increase in this interval, reaching a maximum of 12%, 7%, 5% and 4%, respectively. In this ecozone, the peridinoid dinoflagellate cysts record a significant decrease in the relative abundances of the inner neritic Andalusiella and Deflandrea groups (up to  $\sim 4\%$ ) and

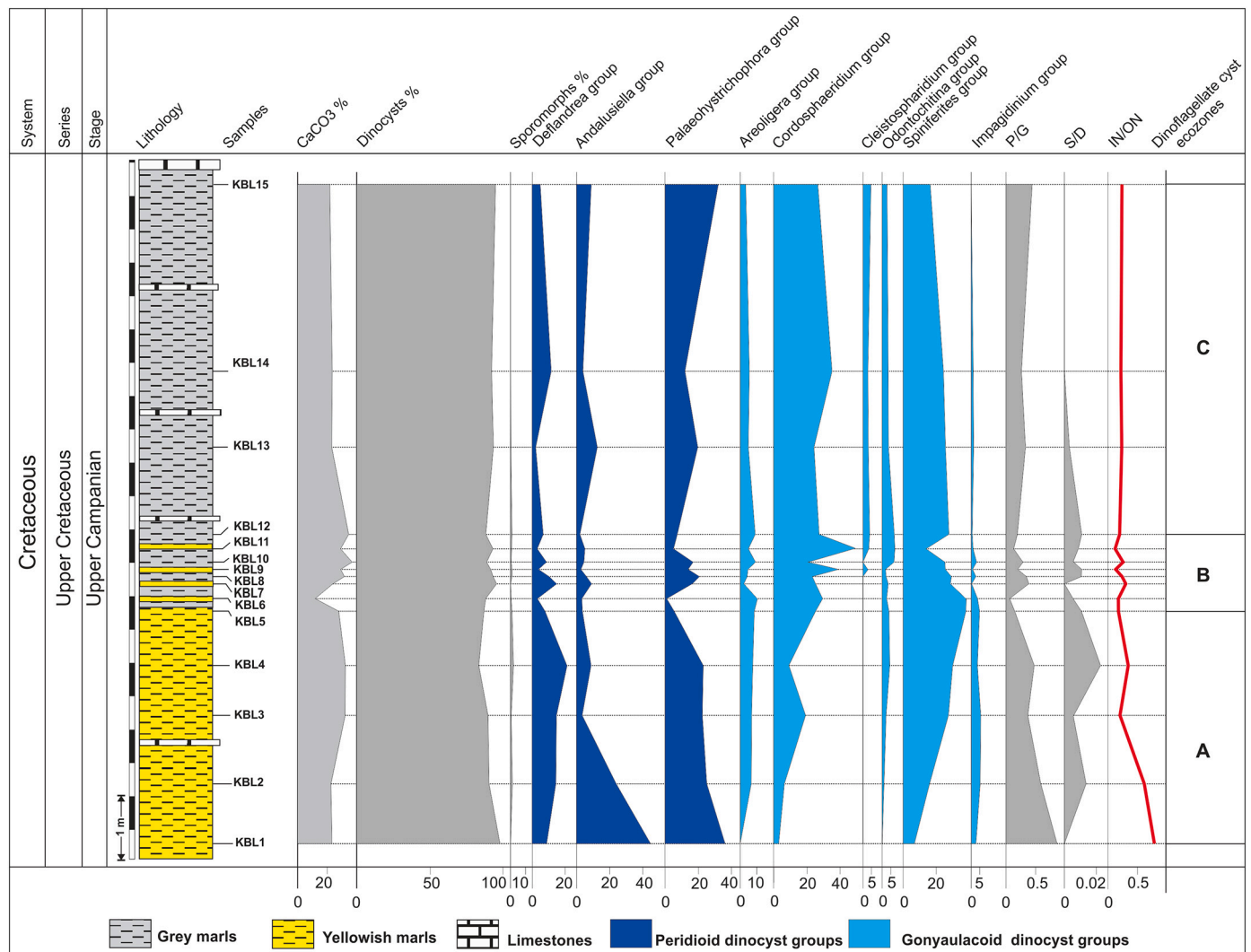


**Fig. 6.** Quantitative results for the paleoenvironmental reconstruction of the upper Campanian marly succession in the Bou Lila section, region of Ksar El-Kébir, western External Rif, northwestern Morocco. Lithology and sample position, calcimetry (CaCO<sub>3</sub>%), relative abundances of selected dinoflagellate cyst groups, percentages of dinoflagellate cysts, percentages of sporomorphs (spores and pollen), peridinioid/gonyaulacoid dinoflagellate cyst ratios (P/G), sporomorph/dinoflagellate cyst (dinoflagellate cyst+marine acritarchs) ratios (S/D), inner neritic dinoflagellate cyst/outer neritic to oceanic dinoflagellate cyst ratios (IN/ON) and ecozones are presented.

*Palaeohystrichophora* group (up to ~2%), associated with a decrease of the P/G ratios (up to 0.1), S/D ratios (up to 0) and IN/ON ratios (up to 0.2). These changes were registered in the basal part of the ecozone B, especially in sample KBL6. All these findings suggest more offshore conditions than the previous ecozone (A), but under a transgressive regime inferred from the increase of the relative abundance of the *Cordosphaeridium* group. The presence of the *Cleistosphaeridium* group, which is indicative of outer neritic conditions (Sluijs et al., 2005) and the oceanic *Impagidinium* group, support the more offshore conditions inferred here from the increase of the relative abundance of the *Cordosphaeridium* and *Spiniferite-Achomosphaera* groups. Furthermore, the *Areoligera-Glyphyrocysta* group, which increased abundance indicates a marine transgression (Brinkhuis, 1994; Stover et al., 1996), records a low abundance (12%), but it is the highest in the base of this interval (sample KBL6), slightly supporting the transgressive regime suggested previously by the *Cordosphaeridium* group. Also, the *Odontochitina* group, which is indicative of near shore marine environment (Wilpshaar and Leereveld, 1994; Leereveld, 1995), records low abundance (<5%) in this ecozone.

This ecozone is characterized by important fluctuations in the relative abundances of the dinoflagellate cyst groups and the P/G, S/D and

IN/ON ratios, which are likely related to a tectonic instability (e.g., discontinuous subsidence) (Slimani et al., 2016), a facies variation (alternating decimetric yellowish and grey marly layers) or fluctuations in the nutrient supply.

### 6.2.3. Ecozone C (sampling interval KBL13–KBL15)

This ecozone corresponds to the grey marls, assigned here to the upper Campanian (upper part). It is characterized by regular relative abundances of the dinoflagellate cyst groups, a dominance of open neritic groups (~60%), mainly the *Spiniferites-Achomosphaera* and *Cordosphaeridium* groups, and by low P/G ( $\leq 0.4$ ), S/D (0%) and IN/ON (0.2) ratios, indicating a stable, outer neritic setting during a transgressive regime.

### 6.3. Palynofacies analysis

Almost all the analyzed samples record very high proportions of dinoflagellate cysts (>90%) of the total palynomorphs (Fig. 4), indicating a normal and a shallow to a deep marine environment (according to Federova, 1977; Durringer and Durringer, 1985; Tyson, 1995).

The projection of counting results of kerogen in the AOM-



Palynomorphs-Phytoclasts ternary diagram (after Tyson, 1995) revealed two palynofacies patterns (clusters A and B) (Fig. 7). The Phytoclast-Palynomorph palynofacies (cluster A) is recorded in two samples (KBL1 and KBL2). It is characterized by a high abundance of lath-shaped and equidimensional opaque phytoclasts (58–60%), sometimes large in size and angular forms (Figs. 7, 9A), as a result of a short transport and supports closer land proximity (see e.g., Radmacher et al., 2020). This palynofacies also includes a moderate abundance of palynomorphs (mostly dinoflagellate cysts) and a low abundance of light-colored granular AOM (marine origin: 3–12%), and therefore is located in fields III of Tyson (1995), indicating a proximal depositional environment.

The Phytoclast-Palynomorph palynofacies (cluster B) occurs in thirteen samples (KBL3 to KBL15) and shows a slight change in the kerogen composition. It is characterized by a moderate to high abundance of palynomorphs (mostly dinoflagellate cysts: 55–80% of the total kerogen; Fig. 8), a moderate amount of phytoclasts (mainly equidimensional opaque phytoclasts small in size and rounded shapes: 20–45%, Fig. 9E, F) and a low abundance of gelified AOM (derived from terrestrial organic matter degraded by bacteria; Fig. 9B) and granular AOM (marine origin, derived from microbial reworking), showing different colors (Fig. 9C, D). According to Valdés et al. (2004) and Ercegovic and Kostić (2006), the color of marine AOM derived from the phytoplankton degradation generally varies from yellow-green under oxic sedimentary conditions in coastal areas, to brown under dysoxic/anoxic conditions in pelagic zones. In our study, the marine AOM identified in the lower part of the section (sampling interval KBL1–KBL4) shows a light color (Fig. 9C), suggesting a more proximal environment for this interval. While in the middle-upper part of the section (KBL5–KBL15 interval), the brown color of the granular AOM particles (Fig. 9D) indicates anoxic/deep-water conditions. Moreover, these offshore conditions/distal setting of the basin during the sedimentation of the sampling interval KBL5–KBL15 are also supported by the kerogen assemblages which include small, equidimensional opaque to semi-opaque phytoclasts, mainly accumulated during transgressive periods of low terrestrial organic matter supply (Habib, 1982).

Summing up, all the palynofacies contents distinguished above, revealed by dinoflagellate cysts, the lath-shaped to equidimensional

opaque phytoclasts distribution and the color of the granular AOM (from yellow to brown), mainly support a proximal depositional environment in the lower part of the section (sampling interval KBL1–KBL4). This environment is followed by a transgressive period and more offshore conditions of the basin during the sedimentation of the middle and upper parts of the studied section. These findings regarding the paleo-environment reconstruction are also in agreement with the interpretation based on dinoflagellate cyst assemblages, described and separated above in three ecozones (refer back to chapter 6.2).

## 7. Discussion

### 7.1. Biostratigraphic correlations

The Bou Lila section belongs to a marly succession assigned to the Upper Cretaceous in the geological map of the Rif Chain 1:500,000 (Suter, 1980a). It is here precisely dated as late Campanian based on FADs or LADs of marker dinoflagellate cyst taxa. These taxa include species, which are accepted as biostratigraphic markers of the late Campanian on the global scale (*Areoligera coronata*, *Areoligera senonensis*, *Cerodinium diebelii*, *Odontochitina costata*, *Odontochitina operculata*, *Odontochitina porifera*, *Senoniasphaera rotundata*, *Trichodinium castanea* subs *castanea*, *Trigonopyxidia ginella*, *Trithyrodinium suspectum*, *Xenascus ceratioides*) (Stover et al., 1996; Slimani, 1995, 2000, 2001a; Antonescu et al., 2001a, 2001b; Schiøler and Wilson, 2001; Williams et al., 2004; Slimani et al., 2011, 2016; Radmacher et al., 2014; Jbari et al., 2020). They are associated with taxa, which are markers of the late Campanian by their FADs, at least in the Tethyan Realm (*Cerodinium boloniense*, *Chatangiella? robusta*, *Pterodinium cretaceum*, *Senegalinium bicavatum*, *Rigaudella appenninica* and *Trithyrodinium evittii* (Soncini, 1990; Williams et al., 1993; Hoek et al., 1996; Slimani et al., 2016; Jbari et al., 2020). Furthermore, other dinoflagellate cyst taxa, recorded in the late Campanian in Europe (Wilson, 1974; Neumann et al., 1983; Foucher, 1985; Masure, 1985; Slimani, 1994, 2001a, 2001b, 2003; Antonescu et al., 2001a, 2001b; Schiøler and Wilson, 2001; Aleksandrova and Zaporozhets, 2008; Slimani et al., 2011; Slimani and Louwye, 2013; Surlyk et al., 2013; Niechwedowicz, 2019), are also found in the Bou Lila section and helped to refine the age of the studied section.

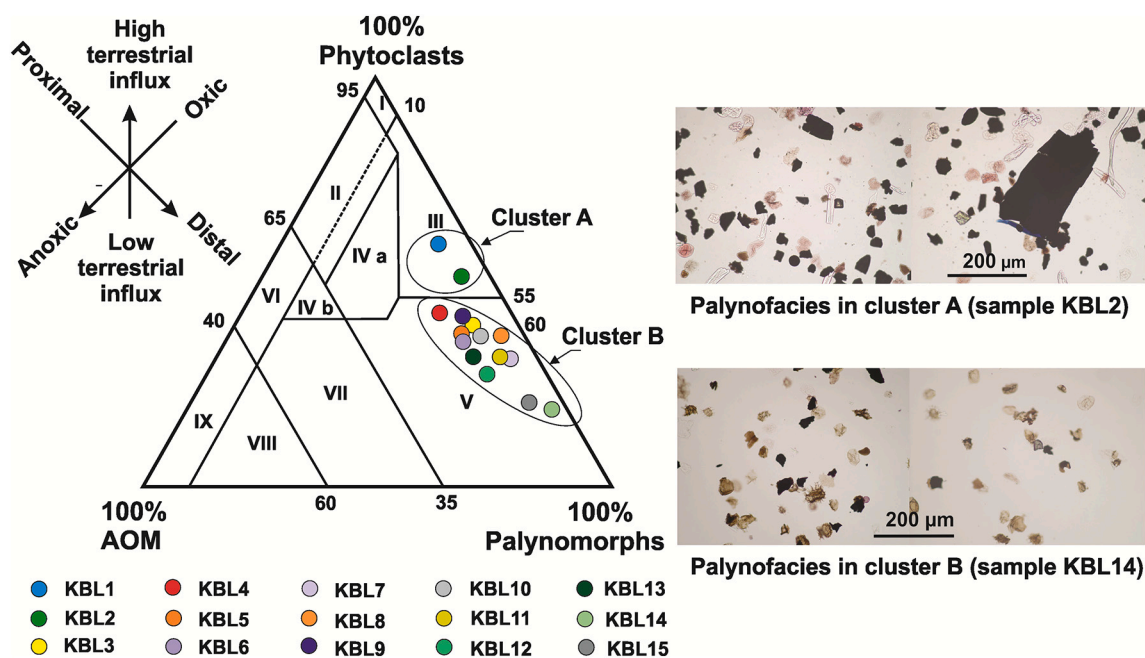


Fig. 7. Ternary kerogen plots (Tyson, 1995) for the upper Campanian deposits, and sample clusters in the Bou Lila section, region of Ksar El-Kébir, western External Rif, northwestern Morocco. Different types of palynofacies are also shown. AOM=amorphous organic matter.

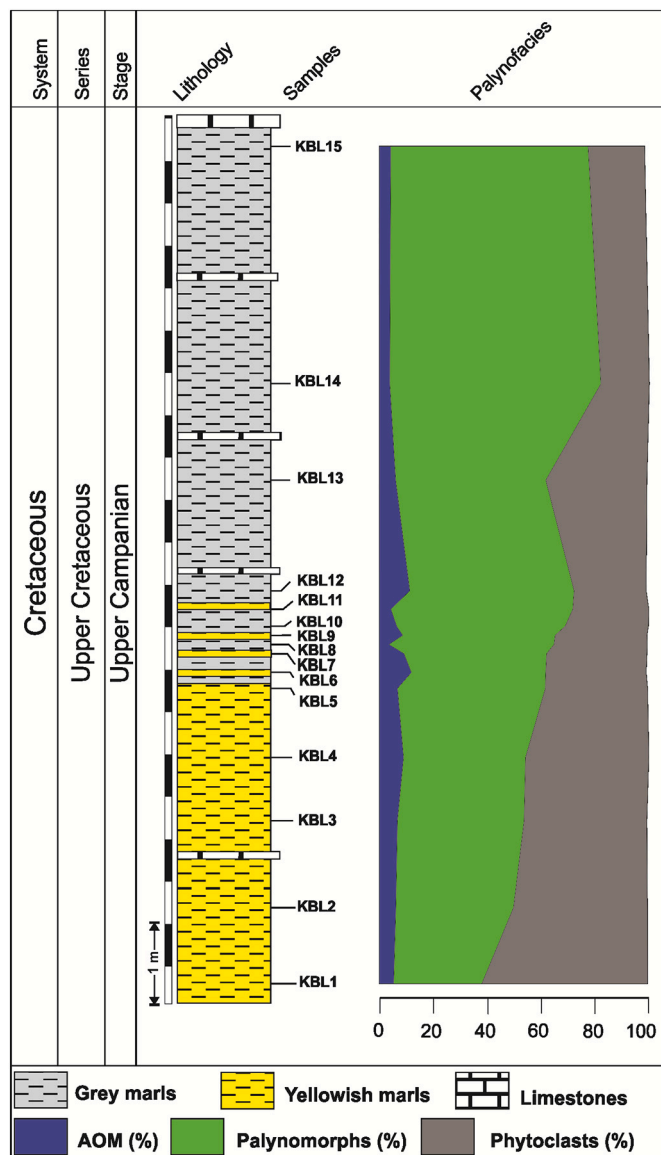


Fig. 8. Stratigraphic distribution of the palynofacies composition: AOM, phytoclasts and palynomorphs.

These species include *Alterbidinium kirschii*, *Apteodinium crassum*, *Areoligera flandriensis*, *Batiacasphaera solida*, *Canninginopsis bretonica*, *Cassiculosphaeridia? intermedia*, *Cribroperidinium wilsonii* subsp. *wilsonii*, *Cyclonephelium filoreticulatum?*, *Exochosphaeridium brevitricatum*, *Impagidinium rigidaseptatum*, *Impagidinium scabrosum*, *Nematosphaeropsis philippotii*, *Raetiaedinium belgicum*, *Raetiaedinium laevigatum*, *Rottnestia wetzeli* subsp. *brevispinosa*, *Palynodinium grillator*, *Senoniasphaera reticulata* in Wilson (1974), *Valensiella foucheri* and *Xenascus wetzeli*. Most of the latter species were recorded for the first time in upper Campanian sequences of the western External Rif, namely the Sekada sequence (Slimani et al., 2016), the Tattofte sequence (Jbari et al., 2020) and in the study outcrop. Thus, the dinoflagellate cyst assemblages of the Bou Lila section are composed of cosmopolitan, Tethyan and many other taxa, which were recorded previously in the late Campanian strata from the type Maastrichtian area and northern Belgium (Wilson, 1974; Foucher, 1985; Slimani, 1994, 1995, 2000, 2001a, 2001b, 2003; Slimani and Louwey, 2013), Denmark (Wilson, 1974; Surlyk et al., 2013), the Campanian type area (Neumann et al., 1983; Masure, 1985) and the GSSP for the base of the Maastrichtian (Antonescu et al., 2001a, 2001b; Schiøler and Wilson, 2001). That means that the dinoflagellate cysts can

be a very useful tool for correlation of the Bou Lila section with Tethyan and also Boreal sections. The lower part of the section (yellowish marls: samples KBL1–KBL4) may be correlatable with the dinoflagellate cyst *Exochosphaeridium? masureae* Zone of Slimani (2001a), calibrated with the Northwest Europe *Belemnitella mucronata* Zone (lower part of the late Campanian). However the middle part (alternated beds of yellowish and grey marls: samples KBL5–KBL11) and the upper part (grey marls: KBL11–KBL15) of the section can be correlated with the dinoflagellate cyst *Areoligera coronata* Zone (middle part of the late Campanian), calibrated with the Northwest Europe *Belemnitella wodii* Zone (Figs. 5, 10).

## 7.2. Paleobiogeography and paleoclimate

From a paleobiogeographic point of view, the Campanian dinoflagellate cyst assemblages in this section are characterized by the occurrence of peridinoid taxa from the temperate province (smaller forms of *Chatangiella*, *Alterbidinium*, *Isabelidinium*, *Trithyrodinium*) and taxa from the tropical province (*Andalusiella*, *Cerodinium*, *Senegalium*), defined by Lentin and Williams (1980), suggesting a mixed subtropical to temperate setting. Similar dinoflagellate cyst assemblages, indicating subtropical to temperate setting, were recorded from the late Campanian and Maastrichtian in Morocco, in the Phosphate Plateau (Soncini, 1990) and Rif Chain (Slimani et al., 2010; Slimani and Toufiq, 2013; Slimani et al., 2016; Jbari et al., 2020). This setting may slightly be different from those recorded at other sites in the southern and eastern Tethyan regions, where dinoflagellate cysts registered a tropical to subtropical setting, such as Tunisia (M'Hamdi et al., 2013, 2014, 2015), Egypt (Soliman and Slimani, 2019; Tahoun and Mohamed, 2020) and Ivory Coast (Guédé et al., 2019). The presence of the northern high-latitude cold-water species *Palynodinium grillator* (Brinkhuis et al., 1998) within the dinoflagellate cyst assemblage of the Bou Lila section may be explained by a southward migration through the Atlantic Ocean, probably related to the short cooling episode during the Campanian–Maastrichtian transition (Barrera and Savin, 1999; Friedrich and Meier, 2006; Thibault et al., 2015, 2016). Similar records of *Palynodinium grillator* have been mentioned in the upper Campanian deposits from the Tattofte section, located ~6 km south of the studied section (Jbari et al., 2020, p. 10). Also, *Palynodinium grillator* has recently been considered to be associated with other factors such as water stratification (Vellekoop et al., 2019).

*Trithyrodinium evittii* is recognized as a warm-water species (Lentin and Williams, 1980; Smit and Brinkhuis, 1996) in the Tethyan province. The late Campanian age of the FAD of *Trithyrodinium evittii*, reported in southern Europe (Antonescu et al., 2001a, 2001b; Schiøler and Wilson, 2001; Skupien and Mohamed, 2008), was confirmed in the Rif Chain (Morocco) by Slimani et al. (2016), Jbari et al. (2020) and used it for the age determination. On the other hand, the FAD of this species is getting younger (crossing the Cretaceous/Paleogene boundary) towards the higher latitudes of both Northern and Southern Hemispheres. The age differences of the FAD of *Trithyrodinium evittii* between the Mediterranean and higher latitude sites suggest of a bipolar migration of this species in response to the global warming during the Late Cretaceous (Smit and Brinkhuis, 1996; Nøhr-Hansen and Dam, 1997; Brinkhuis et al., 1998; Willumsen, 2006). A northward migration can also be suggested here for *Alterbidinium varium* and *Alterbidinium kirschii*. The age of the FAD of these species is late Campanian in the Mediterranean regions and southern Europe (Eshet et al., 1994; Hoek et al., 1996; Antonescu et al., 2001a, 2001b; Schiøler and Wilson, 2001, Slimani et al., 2016; Jbari et al., 2020), but is younger (early Maastrichtian) in northern Europe (Kirsch, 1991; Slimani, 2000, 2001a; Slimani et al., 2011; Surlyk et al., 2013; Țabără et al., 2017).

## 7.3. Paleoenvironments

The paleoenvironmental interpretations in this study are based



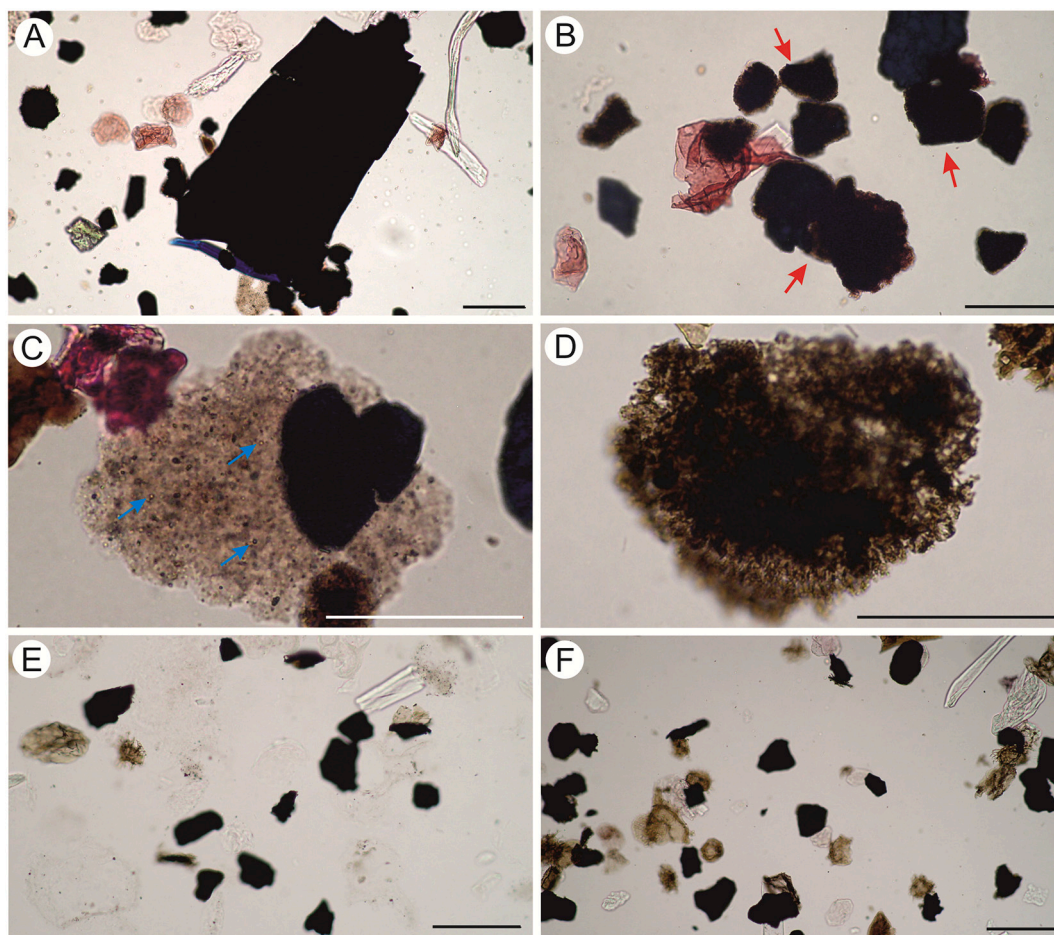


**Fig. 9.** Typical constituents of the different palynodebris groups recognized in the studied samples (all unoxidized residues; scale bar 50  $\mu\text{m}$ ). A. opaque phytoclasts, large in size and angular forms of terrestrial origin (KBL2 sample). B. particles of gelified AOM (continental origin; red arrows; KBL4 sample). C. granular AOM (marine origin) light in color, in association with very small coccoid bodies (bacteria or algae; blue arrows; KBL4 sample). D. dark-brown granular AOM (marine origin; KBL7 sample). E. small equidimensional opaque phytoclasts (KBL10 sample). F. equidimensional opaque phytoclasts small in size and rounded shapes, mixed with numerous dinoflagellate cysts (KBL13 sample).

essentially on fluctuations in the relative abundances of the gonyaulcoid *Spiniferites-Achomosphaera* and *Cordosphaeridium* groups, the peridinioid *Andalusiella* and *Deflandrea* groups and from the P/G, S/D and IN/ON ratios and palynofacies analysis. The paleoenvironmental interpretations inferred from these different quantitative palynological parameters are compared below (Fig. 10):

The lower part of the studied section, corresponding to the yellowish marls, records an inner to intermediate neritic setting (ecozone A), with nearshore conditions in the most basal part of the section. This marine setting is associated with a relatively high productivity, a nutrient supply of continental origin and freshwater conditions favorable for the proliferation of the *Deflandrea* group, inferred from an increase, mainly in the sample KBL4, of S/D ratios and % of the *Deflandrea* group. From the base to the top of this interval (samples KBL1 up to KBL4), the dinoflagellate cyst assemblages show ascending gradual offshore conditions, inferred from ascending progressive increase in the relative abundances of the open neritic *Cordosphaeridium* and *Spiniferites-Achomosphaera* groups and decrease of the shallow neritic *Andalusiella* and *Deflandrea* groups. This environment is also confirmed by the palynofacies analysis, suggesting a proximal depositional environment for the lowermost part of the section, (field III in the AOM-Palynomorphs-Phytoclasts ternary diagram of Tyson, 1995; Figs. 7, 8). Nearshore or oxic sedimentary conditions in coastal area of this interval are also supported by the Kerogen, which consists of a high amount of opaque phytoclasts (sometimes large in size and angular shapes as a result of a

short transport), as well as low proportions of light-colored granular AOM (marine origin).

The middle part of the section, corresponding to the yellowish-grey marly transition, records an intermediate neritic setting (ecozone B) with unstable, but more offshore conditions than the lower part (ecozone A), and a transgressive regime revealed by increasing of the relative abundance of the open neritic *Cordosphaeridium* group was outlined. The unstable conditions are likely related to a tectonic instability or fluctuations of the nutrient supply. The succession of alternating decimetric layers of yellowish and grey marls throughout this part of the section may also confirm such tectonic instability (a short period of a discontinuous subsidence for example). The palynofacies analysis also suggests a more offshore/distal depositional environment, indicated by the palynofacies of field V (in Tyson's, 1995 diagram), which is characterized by high abundance of palynomorphs (57–67%), a moderate abundance of opaque phytoclasts (mainly equidimensional particles; 33–43%) and a low abundance of brown granular AOM (3–12%). Compared to the middle part of the section, the palynofacies analysis suggests here a more distal setting, revealed mainly in the uppermost part of the section (samples KBL14 and KBL15) by a palynofacies of field V with a high abundance of palynomorphs (70–80%) (mostly dinoflagellate cysts) and a low content of phytoclasts (20–30%) and granular AOM (5–7%) (Figs. 7, 8).

From the base to the top of the Bou Lila section, a progressive increase in the frequency of the palynomorphs (essentially dinoflagellate



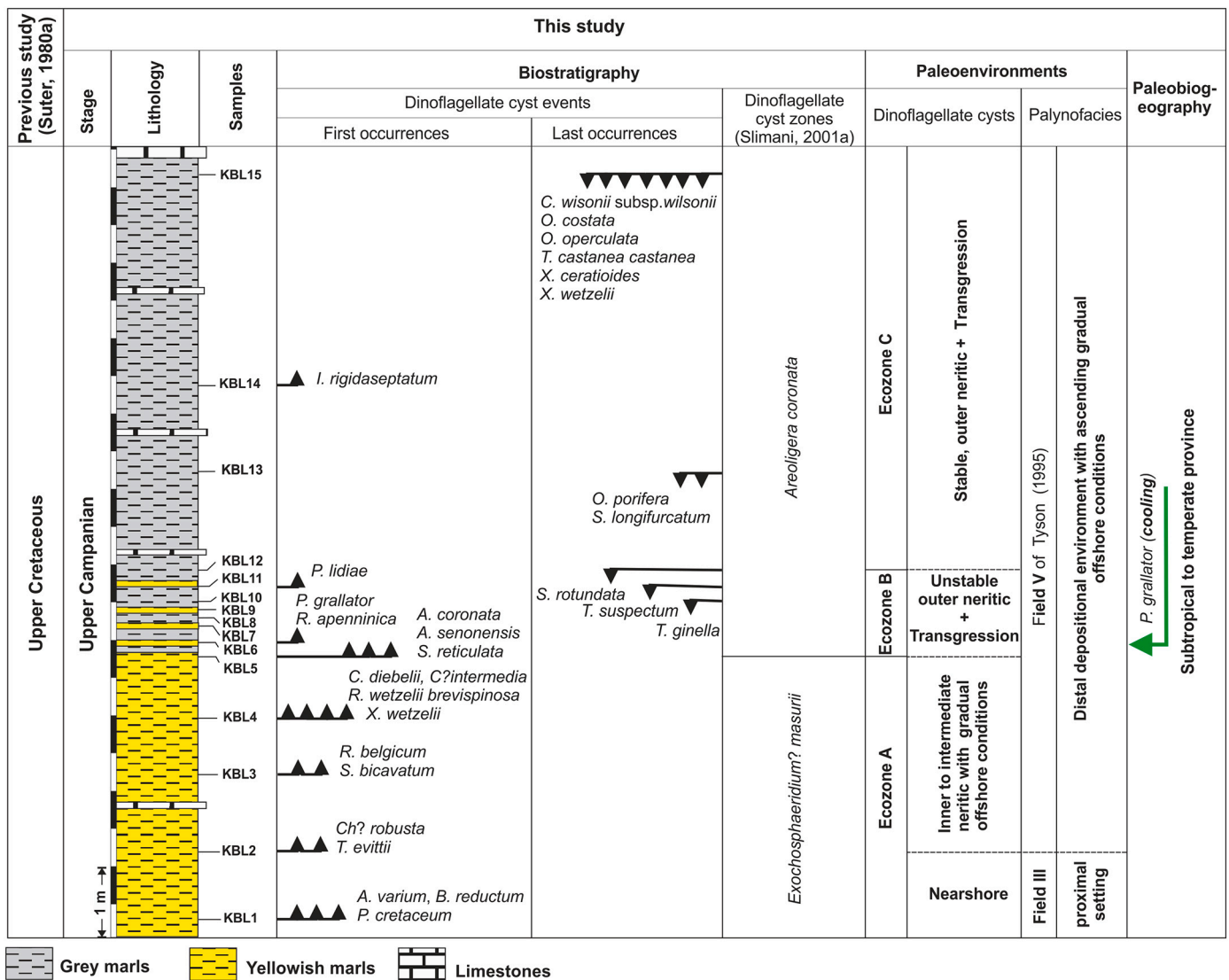


Fig. 10. Recapitulation scheme of the biostratigraphy, paleoenvironments and paleobiogeography in the Bou Lila section, region of Ksar El-Kébir, western External Rif, northwestern Morocco.

cysts) and a decrease in the proportion of the phytoclasts (Figs. 7, 8), suggest ascending gradual offshore conditions, which are similar to those inferred based on the distribution of peridinoid and gonyaulacoid dinoflagellate cyst groups. These environmental changes are likely related to a transgression and probably a progressive subsidence (Fig. 10), and may be related to the third-order sea-level rise UZA-4.3 (High Stand systems tract; HST) of Haq et al. (1988), which is supported by the relative sea level rise inferred from the IN/ON ratios (0.2). Furthermore, this phase of sea-level rise coincides with the first appearance datum of *Palynodinium grillator*, as indicated by Haq et al. (1988), Fig. 3).

8. Conclusions

The study of the palynofacies and dinoflagellate cyst distribution within the Upper Cretaceous deposits of the Bou Lila section, Ksar El-Kébir region (western External Rif Chain, northern Morocco), led to the following conclusions:

1) The section is precisely assigned to the upper Campanian rather than the Upper Cretaceous as presented in the geological map of the Rif Chain (1:500,000), based on FADs and LADs of biostratigraphic

dinoflagellate cyst markers. Biostratigraphic correlations of the section were possible with the upper Campanian dinoflagellate cyst *Exochosphaeridium? masureae* and *Areoligera coronata* zones of Slimani (2001a), calibrated with the Northwest Europe *Belemnitella mucronata* Zone and *Belemnitella wodii* Zone, respectively.

- The studied samples record an ascending gradual change, from an inner neritic setting (or proximal shelf) with nearshore, warm-water and high productivity conditions in the lowermost part of the section to a stable outer neritic setting (distal shelf) in the uppermost part of the section. These gradual changes of the paleoenvironment, inferred from both dinoflagellate cyst distribution and palynofacies composition, are likely related to a transgression and probably a progressive subsidence. They may reflect the third-order sea-level rise UZA-4.3 (High Stand systems tract; HST) of Haq et al. (1988). The middle part of the section, corresponding to the yellowish-grey marly transition, records unstable marine conditions, inferred from important fluctuations in the relative abundances of the dinoflagellate cyst groups, which may be related to a tectonic instability or fluctuations in the nutrient supply.
- According to Lentin and Williams (1980), the sediments were deposited in a subtropical to temperate setting, indicated essentially by a peridinoid assemblage belonging to temperate and tropical

provinces. Nevertheless, many studies show that peridinioids are known also from subpolar regions and they may rather be associated with increased nutrient availability than climatic provinces. The presence of the northern high-latitude cold-water species *Palyndinium grillator* in this setting may be explained by a southward migration, probably related to a short cooling episode during the late Campanian. But also, this species may be associated with other factors as water stratification. These inferences between paleoenvironmental and paleobiogeographical interpretations remain to be debated.

#### Declaration of competing interest

No conflict of interest was reported by authors.

#### Acknowledgments

The authors thank the Department of Earth Science and the Laboratory of Geo-Biodiversity and Natural Patrimony (“Geophysics, Natural Patrimony and Green Chemistry” Research Center), Scientific Institute, Rabat (Morocco) for the technical help. The journal Editor-in-Chief Ric Jordan and the reviewers Manuel Vieira and an anonymous scientist are kindly thanked for their critical and constructive reviews that enhanced the initial manuscript.

#### Statement

No statement from the authors.

#### Appendix A. Dinoflagellate cyst taxa listed alphabetically by genera, Bou Lila section (western external Rif in Morocco)

All dinoflagellate cyst taxa recorded in the Bou Lila section (western External Rif in Morocco) are listed alphabetically by genera and all species are followed by references of their authors (following Williams et al., 2017: DINOFLAJ3) and where possible by plate and figure references in brackets

6. *Alterbidinium acutulium* (Wilson, 1967b) Lentin and Williams, 1985 (Plate 3, Fig. 9)
22. *Alterbidinium kirschii* Slimani, 1994 (Plate 3, Fig. 6)
7. *Alterbidinium minus* (Alberti, 1959b) Lentin and Williams, 1985
8. *Alterbidinium varium* Kirsch, 1991 (Plate 3, Fig. 1)
24. *Andalusiella gabonensis* (Stover and Evitt, 1978) Wrenn and Hart, 1988
34. *Andalusiella ivoirensis* Masare et al., 1996 (Plate 4, Fig. 9)
23. *Andalusiella mauthei* subsp. *punctata* (Jain and Millepie, 1973) Masare et al., 1996
37. *Andalusiella mauthei* subsp. *mauthei* Riegel, 1974 (Plate 4, Fig. 11)
1. *Andalusiella spicata* (Rauscher and Doubinger, 1982) Lentin and Williams, 1985 (Plate 4, Fig. 10)
76. *Apteodinium crassum* Slimani and Louwy, 2013 (Plate 3, Figs. 17, 18)
5. *Apteodinium deflandrei* (Clarke and Verdier, 1967) Lucas-Clark, 1987 (Plate 3, Fig. 14)
53. *Areoligera coronata* (Wetzel, 1933b) Lejeune-Carpentier, 1938a (Plate 2, Fig. 7)
56. *Areoligera flandriensis* Slimani, 1994
54. *Areoligera senonensis* Lejeune-Carpentier, 1938a (Plate 2, Fig. 8)
77. *Batiacasphaera solida* Slimani, 2003 (Plate 2, Fig. 1)
9. *Biconidinium reductum* (May, 1980) Kirsch, 1991 (Plate 4, Figs. 1, 2)
44. *Canninginopsis bretonica* Marshall, 1990b (Plate 2, Fig. 4)
45. *Cannosphaeropsis utinensis* Wetzel, 1933b (Plate 1, Fig. 20)
46. *Cassiculosphaeridia? intermedia* Slimani, 1994 (Plate 2, Fig. 15)
25. *Cerodinium boloniense* (Riegel, 1974) Lentin and Williams, 1989 (Plate 3, Fig. 5)

47. *Cerodinium diebelii* (Alberti, 1959b) Lentin and Williams, 1987 (Plate 3, Fig. 8)
26. *Cerodinium leptodermum* (Vozzhennikova, 1963) Lentin and Williams, 1987
71. *Chatangiella ditissima* (McIntyre, 1975) Lentin and Williams, 1976
61. *Chatangiella madura* Lentin and Williams, 1976 (Plate 3, Fig. 4)
28. *Chatangiella? robusta* (Benson, 1976) Stover and Evitt, 1978 (Plate 3, Fig. 7; Plate 4, Fig. 12)
10. *Circulodinium distinctum* subsp. *distinctum* (Deflandre and Cookson, 1955) Jansonius, 1986 (Plate 2, Fig. 9)
43. *Codoniella campanulata* (Cookson and Eisenack, 1960a) Downie and Sarjeant, 1965 (Plate 3, Fig. 25)
11. *Coronifera oceanica* Cookson and Eisenack, 1958 (Plate 1, Fig. 10)
31. *Cribroperidinium cooksoniae* Norvick, 1976 (Plate 3, Fig. 22)
12. *Cribroperidinium graemei* Williams et al., 1998 (Plate 3, Fig. 19)
38. *Cribroperidinium wilsonii* subsp. *wilsonii* (Yun Hyesu, 1981) Poulsen, 1996 (Plate 3, 23, 24)
30. *Cyclonephelium filoreticulatum?* Slimani, 1994 (Plate 2, Figs. 5, 6)
74. *Dipythes colligerum* (Deflandre and Cookson, 1955) Cookson, 1965a (Plate 1, Fig. 3)
13. *Dinogymnium digitus* (Deflandre, 1936b) Evitt et al., 1967
14. *Elytrocysta druggii* Stover and Evitt, 1978
69. *Exochosphaeridium brevitruncatum* Slimani, 1994 (Plate 3, Fig. 20)
48. *Florentinia aculeata* Kirsch, 1991 (Plate 1, Fig. 2)
49. *Florentinia ferox* (Deflandre, 1937b) Duxbury, 1980 (Plate 1, Fig. 8)
51. *Glaphyrocysta wilsonii* Kirsch, 1991 (Plate 2, Fig. 17)
78. *Heterosphaeridium heteracanthum* subsp. *heteracanthum* Deflandre and Cookson, 1955 (Plate 2, Fig. 10)
68. *Hystrichodinium pulchrum* Deflandre, 1935 (Plate 1, Fig. 9)
32. *Impagidinium cristatum* (May, 1980) Lentin and Williams, 1981 (Plate 1, Fig. 12)
75. *Impagidinium scabrosum* Slimani, 1994
79. *Impagidinium rigidaseptatum* Slimani, 1994 (Plate 1, Figs. 17–19)
62. *Impagidinium* sp. of Slimani et al. (2016) (Plate 1, Fig. 13)
39. *Isabelidinium cooksoniae* (Alberti, 1959b) Lentin and Williams, 1977a (Plate 3, Fig. 12)
15. *Isabelidinium cretaceum* (Cookson, 1956) Lentin and Williams, 1977a (Plate 3, Fig. 11)
16. *Isabelidinium variabile* Marshall, 1988 (Plate 3, Fig. 10)
2. *Nelsoniella aceras* Cookson and Eisenack, 1960a (Plate 3, Fig. 13)
57. *Nematosphaeropsis philippotii* (Deflandre, 1947a) de Coninck, 1969
58. *Nematosphaeropsis* sp. cf. *lativittata* Wrenn, 1988 (Plate 1, Figs. 15, 16)
17. *Odontochitina costata* Alberti, 1961 (Plate 4, Fig. 5)
29. *Odontochitina operculata* (Wetzel, 1933a) Deflandre and Cookson, 1955 (Plate 4, Fig. 6)
27. *Odontochitina porifera* Cookson, 1956 (Plate 4, Fig. 4)
73. *Palaeocystodinium lidiae* (Górka, 1963) Davey 1969b (Plate 4, Fig. 3)
18. *Palaeohystrichophora infusorioides* Deflandre, 1935 (Plate 3, Fig. 2)
66. *Palyndinium grillator* Gocht, 1970a (Plate 2, Fig. 16)
52. *Phelodinium magnificum* (Stanley, 1965) Stover and Evitt, 1978
19. *Pterodinium cretaceum* Slimani et al., 2008 (Plate 1, Fig. 11)
40. *Raetiaedinium belgicum* Slimani, 1994 (Plate 1, Figs. 5, 6)
63. *Raetiaedinium laevigatum* Slimani, 1994
65. *Rigaudella apenninica* (Corradini, 1973) Below, 1982b (Plate 4, Fig. 14)
41. *Rottnestia wetzelii* subsp. *brevispinosa* Slimani, 1994 (Plate 1, Fig. 7)
35. *Senegalinium bicavatum* Jain and Millepie, 1973 (Plate 3, Fig. 3)
64. *Senoniasphaera alveolata* in Wilson (1974)
4. *Senoniasphaera protrusa* Clarke and Verdier, 1967

55. *Senoniasphaera reticulata* in Wilson (1974) (Plate 2, Figs. 13, 14)
42. *Senoniasphaera rotundata* Clarke and Verdier, 1967 (Plate 2, Fig. 12)
36. *Surculosphaeridium longifurcatum* (Firtion, 1952) Davey et al., 1966 (Plate 1, Fig. 1)
67. *Tanyosphaeridium xanthiopyxides* (Wetzel, 1933b) Stover and Evitt, 1978 (Plate 1, Fig. 4)
20. *Trichodinium castanea* subsp. *castanea* Deflandre, 1935 ex Clarke and Verdier, 1967 (Plate 3, Fig. 15)
70. *Trigonopyxidia ginella* (Cookson and Eisenack, 1960a) Downie and Sarjeant, 1965 (Plate 3, Fig. 27).
33. *Trithyrodinium evittii* Drugg, 1967 (Plate 3, Fig. 16)
3. *Trithyrodinium suspectum* (Manum and Cookson, 1964) Davey, 1969b (Plate 3, Fig. 21)
21. *Turnhosphaera hypoflata* (Yun Hyesu, 1981) Slimani, 1994 (Plate 2, Fig. 11)
59. *Unipontidinium grande* (Davey, 1975) Wrenn, 1988 (Plate 1, Fig. 14)
72. *Valensiella foucheri* Slimani, 1994 (Plate 2, Figs. 2, 3)
60. *Xenascus ceratioides* (Deflandre, 1937b) Lentin and Williams, 1973 (Plate 4, Fig. 13)
50. *Xenascus wetzelii* Slimani, 1996 (Plate 4, Figs., 7, 8)

## References

- AFNOR, 1996. Détermination de la teneur en carbonate - Méthode du calcimètre (Determination of the Carbonate Content - Calcimeter Method). French Association for Normalization, Paris. NF P 94-048.
- Aleksandrova, G.N., Zaporozhets, N.I., 2008. Palynological Characteristics of Upper Cretaceous and Paleogene Deposits on the West of the Sambian Peninsula (Kaliningrad Region), Part 1. Stratigr. Geol. Correl. 16 (3), 295–316.
- Antonescu, E., Foucher, J.C., Odin, G.S., 2001a. Chapitre C2c. Les kystes de dinoflagellés de la carrière de tercis les bains (Landes, France). Dev. Palaeontol. Stratigr. 19, 235–252. [https://doi.org/10.1016/S0920-5446\(01\)80026-1](https://doi.org/10.1016/S0920-5446(01)80026-1).
- Antonescu, E., Foucher, J.C., Odin, G.S., Schiøler, P., Siegl-Farkas, A., Wilson, G.J., 2001b. Chapter C2d. Dinoflagellate cysts in the Campanian-Maastrichtian succession of Tercis les Bains (Landes, France), a synthesis. Dev. Palaeontol. Stratigr. 19, 253–264. [https://doi.org/10.1016/S0920-5446\(01\)80027-3](https://doi.org/10.1016/S0920-5446(01)80027-3).
- Atta-Peters, D., Salami, M.B., 2004. Campanian to Paleocene dinoflagellate cyst biostratigraphy from offshore sediments in the Tano Basin, southwestern Ghana. Rev. Esp. Micropaleontol. 36 (2), 305–321.
- Aurisano, R.W., 1989. Upper Cretaceous dinoflagellate biostratigraphy of the subsurface Atlantic Coastal Plain of New Jersey and Delaware, U.S.A. Palynology 13, 143–179. <https://doi.org/10.1080/01916122.1989.9989359>.
- Aurisano, R., Habib, D., 1977. Upper Cretaceous dinoflagellate zonation of the subsurface Toms River section near Toms River, New Jersey. Dev. Palaeontol. Stratigr. 6, 369–387. [https://doi.org/10.1016/S0920-5446\(08\)70360-1](https://doi.org/10.1016/S0920-5446(08)70360-1).
- Barrera, E., Savin, S.M., 1999. Evolution of late Campanian–Maastrichtian marine climates and oceans. In: Sp. Papers-Geol. Soc. Am., pp. 245–282. <https://doi.org/10.1130/0-8137-2332-9.245>.
- Barrón, E.J., 1987. Cretaceous plate tectonic reconstructions. Palaeogeogr. Palaeoclimatol. Palaeoecol. 59, 3–29. [https://doi.org/10.1016/0031-0182\(87\)90071-X](https://doi.org/10.1016/0031-0182(87)90071-X).
- Brinkhuis, H., 1994. Late Eocene to Early Oligocene dinoflagellate cysts from the Priabonian type-area (Northeast Italy): biostratigraphy and paleoenvironmental interpretation. Palaeogeogr. Palaeoclimatol. Palaeoecol. 107 (1), 121–163. [https://doi.org/10.1016/0031-0182\(94\)90168-6](https://doi.org/10.1016/0031-0182(94)90168-6).
- Brinkhuis, H., Powell, A.J., Zevenboom, D., 1992. High-resolution dinoflagellate cyst stratigraphy of the oligocene/miocene transition interval in northwest and central Italy. In: Neogene and Quaternary Dinoflagellate Cysts and Acritarchs. American Association of Stratigraphic Palynology Foundation, Dallas, pp. 219–258.
- Brinkhuis, H., Bujak, J.P., Smit, J., Versteegh, G.J.M., Visscher, H., 1998. Dinoflagellate-based sea surface temperature reconstructions across the Cretaceous–Tertiary boundary. Palaeogeogr. Palaeoclimatol. Palaeoecol. 141 (1–2), 67–83. [https://doi.org/10.1016/S0031-0182\(98\)00004-2](https://doi.org/10.1016/S0031-0182(98)00004-2).
- Carvalho, M.A., Bengtson, P., Lana, C.C., 2016. Late Aptian (Cretaceous) paleoceanography of the South Atlantic Ocean inferred from dinocyst communities of the Sergipe Basin, Brazil. Paleoceanography 31, 2–26. <https://doi.org/10.1002/2014PA002772>.
- Chakir, S., Slimani, H., Hssaida, T., Kocsis, L., Gheerbrant, L., Bardet, B., Jalil, N.-E., Mouflih, M., Mahboub, I., Jbari, H., 2020. Dinoflagellate cyst evidence for the age, paleoenvironment and paleoclimate of a new Cretaceous–Paleogene (K/Pg) boundary section at the Bou Angueur syncline, Middle Atlas, Morocco. Cretac. Res. 106, 104221. <https://doi.org/10.1016/j.cretres.2019.104219>.
- Chalouan, A., Michard, A., Feinberg, H., Montigny, R., Saddiqi, O., 2001. The Rif Mountain building (Morocco): a new tectonic scenario. Bull. Soc. Geol. Fr. 172, 603–616. <https://doi.org/10.2113/172.5.603>.
- Chekar, M., Slimani, H., Guédé, K.É., Aassoumi, H., Asebriy, L., 2016. Biostratigraphie des kystes de dinoflagellés et paléoenvironnements dans l'Éocène de la coupe d'Ibn Batouta, région de Tanger, Rif Externe occidentale, Maroc. Ann. Paléontol. 102 (2), 79–93. <https://doi.org/10.1016/j.annpal.2016.05.001>.
- Chekar, M., Slimani, H., Jbari, H., Guédé, K.É., Mahboub, I., Asebriy, L., Aassoumi, H., 2018. Eocene to Oligocene dinoflagellate cysts from the Tattofte section, western External Rif, northwestern Morocco: biostratigraphy, paleoenvironments and paleoclimate. Palaeogeogr. Palaeoclimatol. Palaeoecol. 507, 97–114. <https://doi.org/10.1016/j.palaeo.2018.07.004>.
- Christensen, W.K., 1995. *Belmitella* faunas from the Upper Campanian and Lower Maastrichtian chalk of Norfolk, England. Special Papers in Palaeontology 51, 48 pp.
- Christensen, W.K., 1999. Upper Campanian and Lower Maastrichtian belemnites from the Mons Basin, Belgium. Bulletin de l'Institut Royal des Sciences Naturelles de Belgique, Sciences de la Terre 69, 97–131.
- Corradini, D., 1973. Non-calcareous microplankton from the Upper Cretaceous of the northern Apennines. Boll. Soc. Paleontol. Ital. 11, 119–197.
- Costa, L.L., Davey, R.J., 1992. Dinoflagellate cysts of the Cretaceous System. A stratigraphic index of dinoflagellate cysts, pp. 99–153.
- Düringer, P., Döbinger, J., 1985. La palynologie: un outil de caractérisation des faciès marins et continentaux à la limite Muschelkalk Supérieure Lettenkohle. Sci. Géol. Bull. (Strasbourg) 38, 19–34.
- El Beialy, S.Y., 1995. Campanian-Maastrichtian palynomorphs from the Duwi (Phosphate) Formation of the Hamrawein and Umm El Hueitat mines, Red Sea Coast, Egypt. Rev. Palaeobot. Palynol. 85, 303–317. [https://doi.org/10.1016/0034-6667\(94\)00121](https://doi.org/10.1016/0034-6667(94)00121).
- Ercegovic, M., Kostić, A., 2006. Organic facies and palynofacies: nomenclature, classification and applicability for petroleum source rock evaluation. Int. J. Coal Geol. 68, 70–78. <https://doi.org/10.1016/j.coal.2005.11.009>.
- Ernst, G., 1964. Ontogenie, Phylogenie und Stratigraphie der Belemnitenattung *Gonioteuthis* Bayle aus dem nordwestdeutschen Santon/Campan. Fortschritte in der Geologie von Rheinland und Westfalen 7, 113–174.
- Eshet, Y., Almogi-Labin, A., Bein, A., 1994. Dinoflagellate cysts, paleoproductivity and upwelling systems: a Late Cretaceous example from Israel. Mar. Micropaleontol. 23 (3), 231–240. [https://doi.org/10.1016/0377-8398\(94\)90014-0](https://doi.org/10.1016/0377-8398(94)90014-0).
- Federova, V.A., 1977. The significance of the combined use of microphytoplankton, spores, and pollen for differentiation of multi-facies sediments, 70e88. In: Samoïlovich, S.R., Timoshina, N.A. (Eds.), Questions of Phytostatigraphy 398. Trudy Neftyanoi nauchno-issledovatel'skii geologorazvedochnyi Institut (VNIIGRI), Leningrad (in Russian).
- Fensome, R.A., Williams, G.L., MacRae, R.A., 2009. Late Cretaceous and Cenozoic fossil dinoflagellates and other palynomorphs from the scotian margin, offshore eastern Canada. J. Syst. Palaeontol. 7 (1), 1–79. <https://doi.org/10.1017/S1477201908002538>.
- Fensome, R.A., Nøhr-Hansen, H., Williams, G.L., 2016. Cretaceous and Cenozoic dinoflagellate cysts and other palynomorphs from the western and eastern margins of the Labrador-Baffin Seaway. Geol. Surv. Denmark Greenl. Bull. 36, 143 pp.
- Foucher, J.-C., 1976. Dinoflagellés et acritarches des silices crétaées du Bassin de Paris: une synthèse stratigraphique. Ann. Univ. A.R.E.R.S., Reims, 1975, 13: 8–10.
- Foucher, J.-C., 1979. Distribution stratigraphique des kystes de dinoflagellés et des acritarches dans le Crétacé Supérieur du Bassin de Paris et de l'Europe septentrionale. Palaeontogr. Abt. B 169, 78–105.
- Foucher, J.-C., 1983. Les dinokystes des craies campano-maastrichtiennes de Hallembaye (Belgique) et de Beutenaken (Pays-Bas). In: Inventaire et répartition stratigraphique. VIIème Symposium de l'Association de Palynologues de la Langue Française, Paris, 10–12 septembre 1983, 2 pp.
- Foucher, J.-C., 1985. Dinoflagellates. In: Robaszynski, F., Bless, M.J.M., Felder, P.J.S., Foucher, J.-C., Legoux, O., Manivit, H., Messen, J.P.M.Th., Van der Tuuk, L.A. (Eds.), The Campanian-Maastrichtian Boundary in the Chalky Facies Close to the Type-Maastrichtian Area, Bul. C. R. Explor.-Prod. Elf-Aquitaine 9 (1), pp. 32–40.
- Friedrich, O., Meier, K.S., 2006. Suitability of stable oxygen and carbon isotopes of calcareous dinoflagellate cysts for paleoclimatic studies: evidence from the Campanian/Maastrichtian cooling phase. Palaeogeogr. Palaeoclimatol. Palaeoecol. 239 (3–4), 456–469. <https://doi.org/10.1016/j.palaeo.2006.02.005>.
- Guasti, E., 2005. Early Paleogene Environmental Turnover in the Southern Tethys as Recorded by Foraminiferal and Organic-Walled Dinoflagellate Cysts Assemblages (Ph. D thesis). University of Bremen (203 pp).
- Guédé, K.É., 2016. Etude comparée de la palynoflore (kystes de dinoflagellés) aux passages Crétacé–Paléogène (K–Pg) et Paléogène–Éocène (P–E) du Nord-Ouest du Maroc et du Sud-Ouest de la Côte d'Ivoire: Systématique, Biostratigraphie, Paléoenvironnements et Paléobiogéographie (PhD thesis). University Mohammed V. Rabat, Morocco, p. 341.
- Guédé, K.É., Slimani, H., Louwye, S., Asebriy, L., Toufiq, A., Ahmamou, M.F., El Amrani El Hassani, I.-E., Digbehi, Z.B., 2014. Organic-walled dinoflagellate cysts from the Upper Cretaceous–lower Paleocene succession in the western External Rif, Morocco: new species and new biostratigraphic results. Geobios 47, 291–304. <https://doi.org/10.1016/j.geobios.2014.06.006>.
- Guédé, K.É., Slimani, H., Chekar, M., M'Hamdi, A., Mouah, R., Digbehi, B.Z., 2019. Late Cretaceous to Early Eocene dinoflagellate cysts from the “12 frères” borehole, Fresco, southwestern Côte d'Ivoire: biostratigraphy and paleobiogeographic implication. J. Afr. Earth Sci. 150, 744–756. <https://doi.org/10.1016/j.jafrearsci.2018.10.003>.
- Guzhikov, A.Yu., Aleksandrova, G.N., Baraboshkin, E.Yu., 2020. New Sedimentological, Magnetostratigraphic, and Palynological Data on the Upper Cretaceous Alan-Kyr Section (Central Crimea). Moscow Univ. Geol. Bul. 75 (1), 20–30. <https://doi.org/10.3103/S0145875220010056>.



- Habib, D., 1982. Sedimentary supply origin of Cretaceous black shales. In: Schlanger, S. O., Cita, M.B. (Eds.), *Nature and Origin of Cretaceous Carbon-rich Facies*. Acad. Press, London, pp. 113–127.
- Habib, D., Miller, J.A., 1989. Dinoflagellate species and organic facies evidence of marine transgression and regression in the Atlantic Coastal Plain. *Palaeogeogr. Palaeoclimatol. Palaeoecol.* 74, 23–47. [https://doi.org/10.1016/0031-0182\(89\)90018-7](https://doi.org/10.1016/0031-0182(89)90018-7).
- Haq, B.D., Hardenbol, J., Vail, P.R., 1988. Mesozoic and Cenozoic chronostratigraphy and cycles of sea-level change. In: Wilgus, C.K., Hastings, B.S. (Eds.), *Sea-Level Changes; An Integrated Approach*, 42. SEPM, Special Publication, pp. 71–108.
- Hay, W.W., 2009. Cretaceous oceans and ocean modeling. *SEPM Spec. Publ.* 91, 243–271.
- Helby, R., Morgan, R., Partridge, A.D., 1987. A palynological zonation of the Australian Mesozoic. In: Jell, P.A. (Ed.), *Studies in Australian Mesozoic Palynology*. Mem. Assoc. Australasian Palaeont., pp. 1–94, 4.
- Hoek, R.P., Eshet, Y., Almogi-Labin, A., 1996. Dinoflagellate cyst zonation of Campanian–Maastrichtian sequences in Israel. *Micropaleontology* 125–150. <https://doi.org/10.2307/1485866>.
- Ioannides, N.S., 1986. Dinoflagellate cysts from Upper Cretaceous–Lower Tertiary sections, Bylot and Devon Islands, Arctic Archipelago. *Geol. Surv. Can.* 371, 1–99.
- Jbari, H., Slimani, H., Chekar, M., Asebriy, L., Benzaggagh, M., Mahboub, I., Chakir, S., 2020. Campanian to Danian dinoflagellate cyst assemblages from the southwestern Tethyan margin (Tattofte section, western External Rif, Morocco): biostratigraphic and paleobiogeographic interpretations. *Rev. Palaeobot. Palynol.* 279, 104225 <https://doi.org/10.1016/j.revpalbo.2020.104225>.
- Keutgen, N., Van der Tuuk, L.A., 1990. Belemnites from the Lower Maastrichtien of Limbourg, Aachen and Liège. *Meded. Rijks Geol. Dienst* 44, 1–29.
- Kirsch, K.-H., 1991. Dinoflagellatenzysten aus der Oberkreide des Helvetikums und Nordultrahelvetikums von Oberbayern. *Münchner. Geowissenschaftliche Abhandlungen, Reihe A. Geol. Paläontol.* 22, 1–306.
- Lebedeva, N.K., Kuzmina, O.B., Soboleva, E.S., Khazina, I.V., 2017. Stratigraphy of Upper Cretaceous and Cenozoic deposits of the Bakchar iron ore deposit (southwestern Siberia): new data. *Stratigr. Geol. Correl.* 25, 76–98.
- Leblanc, D., 1975–1979. Etude géologique du Rif externe oriental au nord de Taza (Maroc). Notes et Mémoires du Service Géologique du Maroc. 281, 1–159.
- Leereveld, H., 1995. Dinoflagellate Cysts from the Lower Cretaceous Río Argos Succession (SE Spain): (met Een Samenvatting in Het Nederlands): Proefschrift Ter Verrijving Van de Graad Van Doctor Aan de Universiteit de Utrecht (...). LPP Foundation.
- Lentin, J.K., Williams, G.L., 1980. Dinoflagellate provincialism. In: *Am. Assoc. Stratigr. Palynol. Found. Contrib. Ser.*, Vol. 17, pp. 1–47.
- Louwyé, S., 1991. De Dinophyceae uit het Boven-Krijt van West-Belgie: Systematiek, Biostratigraphie. Ph.D. Thesis. Laboratorium voor Paleontologie, Rijksuniversiteit Ghent, 289 pp.
- Luyendyk, B.P., Forsyth, D., Phillips, J.D., 1972. Experimental approach to the paleocirculation of the oceanic surface waters. *Geol. Soc. Am. Bull.* 83 (9), 2649–2664. [https://doi.org/10.1130/0016-7606\(1972\)83\[2649:EATTPJ\]2.0.CO;2](https://doi.org/10.1130/0016-7606(1972)83[2649:EATTPJ]2.0.CO;2).
- M'Hamdi, A., Slimani, H., Ismail-Latrache, K.B., Soussi, M., 2013. Biostratigraphie des kystes de dinoflagellés de la limite Crétacé–Paléogène à Ellès, Tunisie. *Rev. Micropaleontol.* 56 (1), 27–42. <https://doi.org/10.1016/j.revmic.2012.12.001>.
- M'Hamdi, A., Slimani, H., Ismail-Latrache, K.B., Ali, W.B., 2014. Dinoflagellate cysts, palynofacies and organic geochemistry of the Cretaceous–Palaeogene (K–Pg) boundary transition at the Elles section, northeastern Tunisia. *Ann. Soc. Geol. Pol.* 84, 235–247.
- M'Hamdi, A., Slimani, H., Louwyé, S., Soussi, M., Ismail-Latrache, K.B., Ali, W.B., 2015. Les kystes de dinoflagellés et palynofacies de la transition Maastrichtien–Danien du stratotype El kef (Tunisie). *C. R. Palevol.* 14 (3), 167–180. <https://doi.org/10.1016/j.crpv.2015.01.008>.
- Mahboub, I., Slimani, H., 2020. Middle Eocene dinoflagellate cysts from the Tsoul section, eastern External Rif, Morocco: biostratigraphy and paleoenvironmental interpretations. *Arab. J. Geosci.* 13, 197. <https://doi.org/10.1007/s12517-020-5165-7>.
- Mahboub, I., Slimani, H., Toufiq, A., Chekar, M., Djaja, K.L., Jbari, H., Chakir, S., 2019. Middle Eocene to early Oligocene dinoflagellate cyst biostratigraphy and paleoenvironmental interpretations of the Ben Attaya section at Taza, eastern External Rif, Morocco. *J. Afr. Earth Sci.* 149, 154–169. <https://doi.org/10.1016/j.jafrearsci.2018.08.006>.
- Makled, W.A., Mostafa, T.F., Maky, A.B.F., 2014. Mechanism of Late Campanian–Early Maastrichtian oil shale deposition and its sequence stratigraphy implications inferred from the palynological and geochemical analysis. *Egypt. J. Pet.* 23 (4), 427–444. <https://doi.org/10.1016/j.ejpe.2014.09.011>.
- Marheinecke, U., 1992. Monographie der Dinozysten, Acritarcha und Chlorophyta des Maastrichtium von Hemmoor (Niedersachsen). *Palaeontogr. Abt. B* 227, 1–173.
- Masure, E., 1985. Le Campanien stratotypique. étude lithologique et micropaléontologique. In: Neumann, N., Platel, J.P., Andreieff, P., Bellier, J.-P., Damotte, R., Lambert, B., Masure, E., Monciardini, C. (Eds.), *Géologie Méditerranéenne*, 10 (3–4), pp. 41–57.
- Masure, E., Rauscher, R., Dejaj, J., Schuler, M., Ferre, B., 1998. Cretaceous–Paleocene palynology from the Côte D'Ivoire-Ghana transform margin, Sites 959, 960, 961, and 962. In: Mascle, J., Lohmann, G.P., Moulade, M. (Eds.), *Proceedings of the Ocean Drilling Program. Sci. Results*, pp. 253–276. <https://doi.org/10.2973/odp.proc.sr.159.040.1998>.
- May, F.E., 1980. Dinoflagellate cysts of the Gymnodiniaceae, Peridiniaceae, and Gonyaulacaceae from the Upper Cretaceous Monmouth Group, Atlantic Highlands, New Jersey. *Palaeontogr. B* 10–116.
- McArthur, A.D., Gamberi, F., Kneller, B.C., Wakefield, M.I., Souza, P.A., Kuchle, J., 2017. Palynofacies classification of submarine fan depositional environments: outcrop examples from the Marnoso-Arenacea Formation, Italy. *Mar. Pet. Geol.* 88, 181–199. <https://doi.org/10.1016/j.marpetgeo.2017.08.018>.
- McIntyre, O.J., 1975. Morphologie changes in *Deflandrea* from a Campanian section, District of Mackenzie, N.W.T., Canada. *Geosci. Man* 11, 61–76.
- McLachlan, S.M., Pospelova, V., Hebda, R.J., 2018. Dinoflagellate cysts from the upper Campanian (Upper Cretaceous) of Hornby Island, British Columbia, Canada, with implications for Nanaimo Group biostratigraphy and paleoenvironmental reconstructions. *Mar. Micropaleontol.* 145, 1–20. <https://doi.org/10.1016/j.marmicro.2018.10.002>.
- Mendonça Filho, J.G., Menezes, T.R., Mendonça, J.O., 2011. Organic Composition (Palynofacies Analysis) (Chapter 5). ICCP Training Course on Dispersed Organic Matter, pp. 33–81.
- Michard, A., Chalouan, A., Feinberg, H., Goffé, B., Montigny, R., 2002. How does the Alpine belt end between Spain and Morocco? *Bull. Soc. Géol. Fr.* 173 (1), 3–15. <https://doi.org/10.2113/173.1.3>.
- Michard, A., De Lamotte, D.F., Saddiqi, O., Chalouan, A., 2008. An outline of the geology of Morocco. In: *Continental Evolution: The Geology of Morocco*, pp. 1–31. <https://doi.org/10.1007/978-3-540-77076-3>.
- Michaud, F., 1987. Stratigraphie et paléogéographie du Mésozoïque du Chiapas (sud est du Mexique) (PhD thesis). Univ. Paris VI, p. 277.
- Mohamed, O., Wagreich, M., 2013. Organic-walled dinoflagellate cyst biostratigraphy of the Well Höflin 6 in the Cretaceous–Palaeogene Rhenodanubian Flysch Zone (Vienna Basin, Austria). *Geol. Carpath.* 64, 209–230.
- Neumann, M., Bellier, J.-P., Damotte, R.R., Lambert, B., Masure, E., Monciardini, C., Platel, J.P., Andreieff, P., 1983. Le Campanien stratotypique: étude lithologique et micropaléontologique. *Géol. Médit.* 10 (3–4), 41–57. <https://doi.org/10.3406/geolm.1983.1243>.
- Niechwedowicz, M., 2019. *Odontochitina dilatata* sp. nov. from the Campanian (Upper Cretaceous) of Poland: the importance of wall structure in the taxonomy of selected ceratiacanth dinoflagellate cysts. *Palynology* 19 (3), 423–450. <https://doi.org/10.1080/01916122.2018.1458754>.
- Nøhr-Hansen, H., Dam, G., 1997. Palynology and sedimentology across a new marine Cretaceous/Tertiary boundary section on Nuussuaq, West Greenland. *Geology* 25, 851–854.
- Oboh-Ikenobe, F.E., Yepes, O., Gregg, J.M., 1998. Palynostratigraphy, palynofacies, and thermal maturation of Cretaceous–Paleocene sediments from Côte d'Ivoire-Ghana transform margin. In: Mascle, J., Lohmann, G.P., Moulade, M. (Eds.), *Proceedings of the Ocean Drilling Program, Sci. Res.* 159, pp. 277–318. <https://doi.org/10.2973/odp.proc.sr.159.016.1998>.
- Patriat, P., Segoufin, J., Schlich, R., Goslin, J., Auzéan, J.M., Beuzart, P., Bonnin, J., Olivet, J.L., 1982. Les mouvements relatifs de l'Inde, de l'Afrique et de l'Eurasie. *Bull. Soc. Geol. Fr.* 7, 363–374.
- Pearce, M.A., Jarvis, I., Tocher, B.A., 2009. The Cenomanian/Turonian boundary event, OA2E and paleoenvironmental change in epicontinental seas: new insights from the dinocyst and geochemical records. *Palaeogeogr. Palaeoclimatol. Palaeoecol.* 280, 207–234. <https://doi.org/10.1016/j.palaeo.2009.06.012>.
- Peyrot, D., Barroso-Barcenilla, F., Barrón, E., Comas-Rengifo, M.J., 2011. Palaeoenvironmental analysis of Cenomanian–Turonian dinocyst assemblages from the Castilian Platform (Northern-Central Spain). *Cretac. Res.* 32, 504–526. <https://doi.org/10.1016/j.cretres.2011.03.006>.
- Powell, A.J. (Ed.), 1992. A Stratigraphic Index of Dinoflagellate Cysts. Chapman and Hall, London (290 p).
- Powell, A.J., Brinkhuis, H., Bujak, J.P., 1996. Upper Paleocene–Lower Eocene dinoflagellate cyst sequence biostratigraphy of southeast England. *J. Geol. Soc. Lond. Spec. Publ.* 101 (1), 145–183. <https://doi.org/10.1144/GSL.SP>.
- Prauss, M.L., 2012. The Cenomanian/Turonian Boundary Event (CTBE) at Tarfaya, Morocco, northwest Africa: Eccentricity controlled water column stratification as major factor for total organic carbon (TOC) accumulation: evidence from marine palynology. *Cretac. Res.* 37, 246–260. <https://doi.org/10.1016/j.cretres.2012.04.007>.
- Pross, J., 2001. Dinoflagellate cyst biogeography and biostratigraphy as a tool for palaeoceanographic reconstructions: an example from the Oligocene of western and northwestern Europe. In: Luterbacher, H., Pross, J., Wille, W. (Eds.), *Studies in dinoflagellate cysts in honour of Hans Gocht*, Neues Jahrb. Geol. Paläontol., Abh., pp. 207–219.
- Pross, J., Brinkhuis, H., 2005. Organic-walled dinoflagellate cysts as paleoenvironmental indicators in the Paleogene; a synopsis of concepts. *Palaeontol. Z.* 79 (1), 53–59. <https://doi.org/10.1007/BF03021753>.
- Radmacher, W., Perez-Rodríguez, I., Arz, J.A., Pearce, M.A., 2014. Dinoflagellate biostratigraphy at the Campanian–Maastrichtian boundary in Zumaia, northern Spain. *Cretac. Res.* 51, 309–320. <https://doi.org/10.1016/j.cretres.2014.07.004>.
- Radmacher, W., Kobos, K., Tyszka, J., Jarzyńska, A., Arz, J.A., 2020. Palynological indicators of paleoenvironmental perturbations in the Basque-Cantabrian Basin during the latest Cretaceous (Zumaia, northern Spain). *Mar. Pet. Geol.* 112, 104107. <https://doi.org/10.1016/j.marpetgeo.2019.104107>.
- Riegel, W., 1974. New forms of organic-walled microplankton from an Upper Cretaceous assemblage in southern Spain. *Rev. Esp. Micropaleontol.* 6, 347–366.
- Riegel, W., Sarjeant, W.A.S., 1982. Dinoflagellate cysts from the upper Cretaceous of southern Spain: new morphological and taxonomic observations. *Neues Jahrb. Geol. Paläontol.* 162, 286–303.
- Roncaglia, L., 2002. Lower Maastrichtian dinoflagellates from the Viano Clay Formation at Viano, northern Apennines, Italy. *Cretac. Res.* 23 (1), 65–76. <https://doi.org/10.1006/cres.2002.0298>.

- Roncaglia, L., Corradini, D., 1997. Upper Campanian to Maastrichtian dinoflagellate zonation in northern Apennines, Italy. *Newsl. Stratigr.* 35, 29–57.
- Sánchez-Pellicer, R., Masare, E., Villier, L., 2017. A new biostratigraphic correlation for Late Cretaceous–Paleocene strata of the Gulf of Guinea: evidence from dinoflagellate cysts. *Compt. Rendus Geosci.* 349 (1), 32–41. <https://doi.org/10.1016/j.crte.2016.11.001>.
- Schiøler, P., Wilson, G.J., 1993. Maastrichtian dinoflagellate zonation in the Dan Field, Danish North Sea. *Rev. Palaeobot. Palynol.* 78, 321–351. [https://doi.org/10.1016/0034-6667\(93\)90070-B](https://doi.org/10.1016/0034-6667(93)90070-B).
- Schiøler, P., Wilson, G.J., 2001. Dinoflagellate biostratigraphy around the Campanian–Maastrichtian boundary at Tercis les Bains, southwest France. In: Odin, G.S. (Ed.), *The Campanian–Maastrichtian boundary: characterization and correlation from Tercis-les-Bains (Landes, SW France) to Europe and other continents*, 19, pp. 222–234.
- Schrank, E., 1987. Palaeozoic and Mesozoic palynomorphs from northeast Africa (Egypt and Sudan) with special reference to Late Cretaceous pollen and dinoflagellates. *Berliner Geowiss. Abh.* A 75 (1), 249–310.
- Schrank, E., Ibrahim, M., 1995. Cretaceous (Aptian–Maastrichtian) palynology of foraminifera-dated wells (KRM-1, AG-18) in northwestern Egypt. *Berl. Geowiss. Abh.* A177, 1–44.
- Schumacker-Lambry, J., 1977. Microfossiles végét. aux? planctoniques. In: Streeel, M., Bick, H. (Eds.), *Macro- et microfossiles végétaux dans le contexte litho- et biostratigraphique du Sénonien–Paléocène de la rive gauche de la Meuse au nord de Liège Belgique*. Handout APLF/PK-meeting, Liège, pp. 45–53.
- Schulz, M.-G., 1979. Morphometrisch-variationsstatistische Untersuchungen zur Phylogenie der Belemniten-Gattung *Belemnella* im Untermaastricht NW-Europas. *Geologisches Jahrbuch* A47, 155 pp.
- Setoyama, E., Radmacher, W.B., Kaminski, M.A., Tysz, J., 2013. Foraminiferal and palynological biostratigraphy and biofacies from a Santonian–Campanian submarine fan system in the Vøring Basin (offshore Norway). *Mar. Pet. Geol.* 43, 396–408. <https://doi.org/10.1016/j.marpetgeo.2012.12.007>.
- Skupien, P., Mohamed, O., 2008. Campanian to Maastrichtian palynofacies and dinoflagellate cysts of the Silesian Unit, Outer Western Carpathians, Czech Republic. *Bull. Geosci.* 83, 207–224.
- Slimani, H., 1994. Les dinokystes des craies du Campanien au Danien à Halebay, Turnhout (Belgique) et à Beutenaken (Pays-Bas). In: *Mém. Serv. à l'explication des Cart. géologiques et minières de la Belgique*, Vol. 37, pp. 1–173.
- Slimani, H., 1995. Les dinokystes des craies du Campanien au Danien à Hallembaye et Turnhout (Belgique) et à Beutenaken (Pays-Bas): Biostratigraphie et systématique (PhD thesis). University of Gent, Gent, Belgium, p. 461.
- Slimani, H., 1996. Les dinokystes des Craies du Campanien au Danien à Hallembaye, Turnhout (Belgique) et à Beutenaken (Pays-Bas). *Supplément de systématique*. *Ann. Soc. Géol. Belg.* 117, 371–391. <https://popups.uliege.be/443/0037-9395/index.php?id=2073>.
- Slimani, H., 2000. Nouvelle zonation aux kystes de dinoflagellés du Campanien au Danien dans le Nord et l'Est de la Belgique et dans le Sud-Est des Pays-Bas. *Mem. Geol. Surv. Belg.* 46, 1–88.
- Slimani, H., 2001a. Les kystes de dinoflagellés du Campanien au Danien dans la région de Maastricht (Belgique et Pays-Bas) et de Turnhout (Belgique): biozonation et corrélation avec d'autres régions en Europe occidentale. *Geol. Palaeontol.* 35, 161–201.
- Slimani, H., 2001b. New species of dinoflagellate cysts from the Campanian Danian chalks at Hallembaye and Turnhout (Belgium) and at Beutenaken (The Netherlands). *J. Micropaleontol.* 20, 1–11.
- Slimani, H., 2003. A new genus and two new species of dinoflagellate cysts from the Upper Cretaceous of the Maastrichtian type area and Turnhout (northern Belgium). *Rev. Palaeobot. Palynol.* 126 (3–4), 267–277. [https://doi.org/10.1016/S0034-6667\(03\)00091-5](https://doi.org/10.1016/S0034-6667(03)00091-5).
- Slimani, H., Louwyse, S., 2011. New dinoflagellate cyst species of the *Microdinium* and *Panoradinium* Complexes (Evlitt) from the Upper Cretaceous–Lower Paleogene Chalk Group in the Meer borehole, northern Belgium. *Rev. Palaeobot. Palynol.* 168 (1), 41–50. <https://doi.org/10.1016/j.revpalbo.2011.09.009>.
- Slimani, H., Louwyse, S., 2013. New organic-walled dinoflagellate cyst species from the Upper Cretaceous–Lower Paleogene Chalk Group in the Meer and Turnhout boreholes, Campine Basin, northern Belgium. *Rev. Palaeobot. Palynol.* 192, 10–21. <https://doi.org/10.1016/j.revpalbo.2012.12.001>.
- Slimani, H., Toufiq, A., 2013. A Cretaceous–Paleogene boundary geological site, revealed by planktic foraminifera and dinoflagellate cysts, at Ouled Haddou, eastern external Rif Chain, Morocco. *J. Afr. Earth Sci.* 88, 38–52. <https://doi.org/10.1016/j.jafrearsci.2013.08.008>.
- Slimani, H., Louwyse, S., Toufiq, A., Verniers, J., De Coninck, J., 2008. New dinoflagellate cyst species from Cretaceous/Paleogene boundary deposits at Ouled Haddou, southeastern Rif, Morocco. *Cretac. Res.* 29 (2), 329–344. <https://doi.org/10.1016/j.cretres.2007.06.003>.
- Slimani, H., Louwyse, S., Toufiq, A., 2010. Dinoflagellate cysts from the Cretaceous–Paleogene boundary at Ouled Haddou, Southeastern Rif, Morocco: biostratigraphy, paleoenvironments and paleobiogeography. *Palynology* 34, 90–124. <https://doi.org/10.1080/01916121003629933>.
- Slimani, H., Louwyse, S., Duser, M., Lagrou, D., 2011. Connecting the Chalk Group of the Campine Basin to the dinoflagellate cyst biostratigraphy of the Campanian to Danian in borehole Meer (northern Belgium). *Netherl. J. Geosc.* 90 (2–3), 129–164. <https://doi.org/10.1017/S0016774600001074>.
- Slimani, H., Louwyse, S., Toufiq, A., 2012. New species of organic-walled dinoflagellate cysts from the Maastrichtian–Danian boundary interval at Ouled Haddou, northern Morocco. *Alcheringa* 36, 337–353. <https://doi.org/10.1080/03115518.2012.645629>.
- Slimani, H., Guédé, K.É., Williams, G.L., Asebriy, L., Ahmamou, M., 2016. Campanian to Eocene dinoflagellate cyst biostratigraphy from the Tahar and Sekada sections at Arba Ayacha, western External Rif, Morocco. *Rev. Palaeobot. Palynol.* 228, 26–46. <https://doi.org/10.1016/j.revpalbo.2016.01.003>.
- Slimani, H., Mahboub, I., Toufiq, A., Jbari, H., Chakir, S., Tahiri, A., 2019. Bartonian to Priabonian dinoflagellate cyst biostratigraphy and paleoenvironments of the M'karcha section in the Southern Tethys margin (Rif Chain, Northern Morocco). *Mar. Micropaleontol.* 153, 101785 <https://doi.org/10.1016/j.marmicro.2019.101785>.
- Sluijs, A., Pross, J., Brinkhuis, H., 2005. From greenhouse to icehouse organic-walled dinoflagellate cysts as paleoenvironmental indicators in the Paleogene. *Earth Sci. Rev.* 68, 281–315. <https://doi.org/10.1016/j.earscirev.2004.06.001>.
- Smit, J., Brinkhuis, H., 1996. The Geulhemmerberg Cretaceous/Tertiary boundary section in the Maastrichtian type area, SE Netherlands: summary of results and scenario of events. In: Brinkhuis, H., Smit, J. (Eds.), *The Geulhemmerberg Cretaceous/Tertiary Boundary Section (Maastrichtian Type Area, SE Netherlands)*, *Geol. Mijnb.* 75, pp. 283–293.
- Soliman, A., Slimani, H., 2019. The Cretaceous–Paleogene (K/Pg) boundary in the Dababiya Borehole, southern Egypt: an organic-walled dinoflagellate cyst approach. *Cretac. Res.* 98, 230–249. <https://doi.org/10.1016/j.cretres.2019.02.016>.
- Soncini, M.J., 1990. Palynologie des phosphates des Ouled Abdoun (Maroc). Biostratigraphie et environnements de la phosphatogenèse dans le cadre de la crise Crétacé–Tertiaire. PhD thesis. Institut of Geology, University Louis Pasteur, Strasbourg, France, p. 243.
- Soncini, M.-J., Rauscher, R., 1988. Associations des dinokystes de Maastrichtien–Paléocène phosphaté au Maroc. *Bull. Centres Rech. Explor. Prod. Elf-Aquitaine* 12, 427–450.
- Stover, L.E., Brinkhuis, H., Damassa, S.P., de Verteuil, L., Helby, R.J., Monteil, E., Partridge, A.D., Powell, A.J., Riding, J.B., Smelror, M., Williams, G.L., 1996. Mesozoic–Tertiary dinoflagellates, acritarchs and prasinophytes. In: Jansonius, J., McGregor, D.C. (Eds.), *Palynology: Principles and Applications*, Vol. 2. American Association of Stratigraphic Palynologists Foundation, pp. 641–750.
- Surlyk, F., Rasmussen, S.L., Boussaha, M., Schiøler, P., Schovsbo, N.H., Sheldon, E., Stemmerik, L., Thibault, N., 2013. Upper Campanian–Maastrichtian holostratigraphy of the eastern Danish Basin. *Cretac. Res.* 46, 232–235. <https://doi.org/10.1016/j.cretres.2013.08.006>.
- Suter, G., 1980a. Carte Géologique du Rif au 1/500 000. Notes et Mém. Serv. Géol. Maroc, p. 245a.
- Suter, G., 1980b. Carte structurale du Rif au 1/500 000. Notes et Mém. Serv. Géol. Maroc, p. 245b.
- Tabără, D., Slimani, H., Mare, S., Chira, C.M., 2017. Integrated biostratigraphy and paleoenvironmental interpretation of the Upper Cretaceous to Paleocene succession in the northern Moldavian Domain (Eastern Carpathians, Romania). *Cretac. Res.* 77, 102–123. <https://doi.org/10.1016/j.cretres.2017.04.021>.
- Tahoun, S.S., Mohamed, O., 2020. Distribution of peridiniacean dinoflagellate cysts from cores of organic rich shales of the Duwi and Dakhla formations of Egypt. *J. Afr. Earth Sci.* 170, 103892. <https://doi.org/10.1016/j.jafrearsci.2020>.
- Thibault, N., Gardin, S., 2010. The calcareous nannofossil response to the end-Cretaceous warm event in the Tropical Pacific. *Palaeogeogr. Palaeoclimatol. Palaeoecol.* 291, 239–252. <https://doi.org/10.1016/j.palaeo.2010.02.036>.
- Thibault, N., Anderskov, K., Bjerager, M., Boldreel, L.O., Jelby, M.E., Stemmerik, L., Surlyk, F., 2015. Upper Campanian–Maastrichtian chronostratigraphy of the Skalskor-1 core, Denmark: correlation at the basinal and global scale and implications for changes in sea-surface temperatures. *Lethaia* 48, 549–560. <https://doi.org/10.1111/let.12128>.
- Thibault, N., Harlou, R., Schovsbo, N.H., Stemmerik, L., Surlyk, N., 2016. Late Cretaceous (late Campanian–Maastrichtian) sea-surface temperature record of the Boreal Chalk Sea. *Clim. Past* 12, 429–438. <https://doi.org/10.5194/cp-12-429-2016>.
- Torricelli, S., Amore, M.R., 2003. Dinoflagellate cysts and calcareous nannofossils from the Upper Cretaceous Saraceno Formation (Calabria, Italy): implications about the history of the liguride complex. *Riv. Ital. Paleontol. Stratigr.* 109 (3), 499–516.
- Tyson, R.V., 1995. *Sedimentary Organic Matter: Organic Facies and Palynofacies*. Chapman and Hall, London, 615 pp.
- Valdés, J., Sifeddine, A., Ortlieb, L., Pierre, C., 2004. Interplay between sedimentary organic matter and dissolved oxygen availability in a coastal zone of the Humboldt Current System; Mejillones Bay, northern Chile. *Mar. Geol.* 265, 57–166. <https://doi.org/10.1016/j.margeo.2009.07.004>.
- Vellekoop, J., Woelders, L., Sluijs, A., Miller, K.G., Speijer, R.P., 2019. Phytoplankton community disruption caused by latest Cretaceous global warming. *Biogeosciences* 16 (21), 4201–4210.
- Verbeek, J.W., 1983. The calcareous nannofossils from the Campanian and Maastrichtian rocks of Southern Limburg (The Netherlands) and the adjacent Belgian area. *Bull. Geol. Soc. Den.* 33, 197–200.
- Versteegh, G.J.M., 1994. Recognition of cyclic and non-cyclic environmental changes in the Mediterranean Pliocene: a palynological approach. *Mar. Micropaleontol.* 23, 147–183. [https://doi.org/10.1016/0377-8398\(94\)90005-1](https://doi.org/10.1016/0377-8398(94)90005-1).
- Veira, V., Jolley, D., 2020. Stratigraphic and spatial distribution of palynomorphs in deep-water turbidites: a meta-data study from the Central North Sea Paleogene. *Mar. Pet. Geol.* 104638 <https://doi.org/10.1016/j.marpetgeo.2020.104638>.
- Veira, M., Mahdi, S., Osterloff, P., 2018. New Early Paleocene (Danian) dinoflagellate cyst species from the Ormen Lange Field, Møre Basin, Norwegian Continental Shelf. *Palynology* 42 (2), 180–198. <https://doi.org/10.1080/01916122.2017.1314390>.
- Veira, M., Mahdi, S., Holmes, N., 2020. High resolution biostratigraphic zonation for the UK Central North Sea Paleocene. *Mar. Pet. Geol.* 117, 104400 <https://doi.org/10.1016/j.marpetgeo.2020.104400>.

- Wall, D., Dale, B., Lohmann, G.P., Smith, W.K., 1977. The environmental and climatic distribution of dinoflagellate cysts in modern marine sediments from regions in the North and South Atlantic Oceans and adjacent seas. *Mar. Micropaleontol.* 2, 121–200. [https://doi.org/10.1016/0377-8398\(77\)90008-1](https://doi.org/10.1016/0377-8398(77)90008-1).
- Williams, G.L., Stover, L.E., Kidson, E.J., 1993. Morphology and stratigraphic ranges of selected Mesozoic–Cenozoic dinoflagellate taxa in the Northern Hemisphere. In: *Geol. Surv. Can. Pap.* (92–10) (137 pp.).
- Williams, G.L., Brinkhuis, H., Pearce, M.A., Fensome, R.A., Weegink, J.W., 2004. Southern Ocean and global dinoflagellate cyst events compared: index events for the late Cretaceous–Neogene. In: Exon, N.F., Kennett, J.P., Malone, M.J. (Eds.), *Proceedings of the Ocean Drilling Program, Sci. Results* 189, pp. 1–98. <https://doi.org/10.2973/odp.proc.sr.189.107.2004>.
- Williams, G.L., Fensome, R.A., MacRae, R.A., 2017. DINOFLAJ3. In: *Data Series no. 2 AASP Foundation. The Lentini and Williams index of fossil dinoflagellates 2017 edition. American Association of Stratigraphic Palynologists Contributions Series*, no. 48. <http://dinoflaj.smu.ca/dinoflaj3>.
- Willumsen, P.S., 2006. *Palynodinium minus* sp. nov., a new dinoflagellate cyst from the Cretaceous/Paleogene transition in New Zealand; its significance and palaeoecology. *Cretac. Res.* 27, 954–963. <https://doi.org/10.1016/j.cretres.2006.06.002>.
- Wilpshaar, M., Leereveld, H., 1994. Palaeoenvironmental change in the Early Cretaceous Vocontian Basin (SE France) reflected by dinoflagellate cysts. *Rev. Palaeobot. Palynol.* 84, 121–128. [https://doi.org/10.1016/0034-6667\(94\)90046-9](https://doi.org/10.1016/0034-6667(94)90046-9).
- Wilson, G.J., 1971. A chemical method for the palynological processing of chalk. *Mercian Geol.* 4, 29–36.
- Wilson, G.J., 1974. Upper Campanian and Maastrichtian Dinoflagellate Cysts from the Maastricht Region and Denmark (PhD thesis). University of Nottingham, Nottingham, UK, p. 601.
- Wilson, G.J., 1984. New Zealand Late Jurassic–Eocene dinoflagellate biostratigraphy – a summary. *Newsl. Stratigr.* 13, 104–117.
- Zonneveld, K.A., Marret, F., Versteegh, G.J., Bogus, K., Bonnet, S., Bouimtarhan, I., Crouch, E., de Vernal, A., Elshaniwany, R., Edwards, L., Esper, O., Forke, S., Grøsfjeld, K., Henry, M., Holzwarth, U., Kieft, J.F., Kim, S.Y., Ladouceur, S., Ledu, D., Chen, L., Limoges, A., Londeix, L., Lu, S.H., Mahmoud, M.S., Marino, G., Matsouka, K., Matthiessen, J., Mildenhall, D., Mudie, P., Neil, H., Pospelova, V., Qi, Y., Radi, T., Richerol, T., Rochon, A., Sangiorgi, F., Solignac, S., Turon, J.L., Verleye, T., Wang, Y., Wang, Z., Young, M., 2013. Atlas of modern dinoflagellate cyst distribution based on 2405 data points. *Rev. Palaeobot. Palynol.* 191, 1–197. <https://doi.org/10.1016/j.revpalbo.2012.08.003>.